A Monte Carlo exploration of threefold base geometries for 4d F-theory vacua

Washington Taylor and Yi-Nan Wang

Center for Theoretical Physics, Department of Physics,
Massachusetts Institute of Technology,
77 Massachusetts Avenue, Cambridge, MA 02139, U.S.A.

E-mail: wati@mit.edu, wangyn@mit.edu

Abstract: We use Monte Carlo methods to explore the set of toric threefold bases that support elliptic Calabi-Yau fourfolds for F-theory compactifications to four dimensions, and study the distribution of geometrically non-Higgsable gauge groups, matter, and quiver structure. We estimate the number of distinct threefold bases in the connected set studied to be $\sim 10^{48}$. The distribution of bases peaks around $h^{1,1} \sim 82$. All bases encountered after "thermalization" have some geometric non-Higgsable structure. We find that the number of non-Higgsable gauge group factors grows roughly linearly in $h^{1,1}$ of the threefold base. Typical bases have ~ 6 isolated gauge factors as well as several larger connected clusters of gauge factors with jointly charged matter. Approximately 76% of the bases sampled contain connected two-factor gauge group products of the form $SU(3) \times SU(2)$, which may act as the non-Abelian part of the standard model gauge group. $SU(3) \times SU(2)$ is the third most common connected two-factor product group, following $SU(2) \times SU(2)$ and $G_2 \times SU(2)$, which arise more frequently.

Contents

1 Introduction

F-theory [1–3] provides a powerful and general nonperturbative approach to the construction of large classes of string theory vacua. The construction of an F-theory vacuum in $10 - 2d$ dimensions depends upon a choice of a compactification manifold B that is a complex d-fold. In type IIB language, the axiodilaton of ten-dimensional supergravity encodes an elliptically fibered Calabi-Yau X_{d+1} over the base B. This Calabi-Yau can have singularities corresponding to seven-branes carrying gauge groups and matter in the low-energy $10 - 2d$ dimensional supergravity theory.

In recent years, by focusing on the geometry of the complex surface base B, a fairly complete global picture of the space of 6d F-theory constructions and corresponding elliptic

Calabi-Yau threefolds has been developed [4–10]. At a simplified level, the upshot of this story is that toric bases seem to provide a good representative sample of the set of all possible base surfaces that support elliptic Calabi-Yau threefolds, and that an important part of the basic physics of each base B is captured by the gauge groups and matter in the "non-Higgsable clusters" that are present for a generic elliptic fibration over B.

F-theory compactifications to four space-time dimensions on elliptic Calabi-Yau four-folds present several additional major complications and challenges (see e.g. [11]), including the presence of G-flux, which produces a superpotential that lifts some of the geometric moduli, and world-volume fields on the branes, which can modify the physics of geometrically non-Higgsable structures. Nonetheless, at the level of geometry there are many parallels between the 4d story and the 6d story. As has been found for CY threefolds, the range of possible Hodge numbers for known Calabi-Yau fourfolds seems to be reasonably well captured by elliptic fourfolds over toric threefold bases. And also as found for three-folds, geometrically non-Higgsable gauge groups and matter that are present everywhere in the Weierstrass moduli space of elliptic fibrations over a given base B give a strong guide to the physics and and aid in the classification of 4d F-theory models through the structure of allowed threefold base geometries. Non-Higgsable clusters for base threefolds were studied in specific cases in [12, 13] and systematically analyzed more generally in [14]. In [15], an investigation of the geometry of one large class of threefold bases was carried out, focusing on threefolds with the structure of a $\mathbb{P}^1$-bundle over a complex surface base from among those toric surfaces that themselves support an elliptic CY threefold.

In this paper we carry out a Monte Carlo study of the set of toric threefold bases for 4d F-theory models. The goal of this study is to address some basic questions such as: *How many toric threefolds B support an elliptically fibered Calabi-Yau fourfold? How does the number of geometrically non-Higgsable gauge group factors grow with $h^{1,1}(B)$?*, and: *How typical is the product group* $\mathrm{SU}(3) \times \mathrm{SU}(2)$ *with jointly charged (quark-like) matter as a subgroup of the geometrically non-Higgsable gauge group?* The analysis we perform here is not intended to give a precise statistical analysis of the physical distribution of F-theory vacua or even of the full set of fourfolds. Rather, the goal is to explore a large, potentially characteristic, set of threefold bases to get a general sense of the scope of the set of possibilities and how physical features are distributed. In particular, our approach leaves out some classes of toric threefold bases, specifically those that cannot be reached by a sequence of single blow-ups and blow-downs from the set of bases connected to $\mathbb{P}^3$. The restriction to strictly toric bases also leaves out many bases with E_8 non-Higgsable group factors, which are incorporated more easily in 6d models through a slight extension of the class of toric bases. And we do not address here the classification of G-flux, which would be relevant to analyzing the specific vacua associated with any given fourfold geometry.

Previous explorations of the range of geometries available for 4d F-theory vacua have focused on certain simple classes of elliptic Calabi-Yau fourfolds and threefold bases, in particular threefold bases that are Fano threefolds or $\mathbb{P}^1$ bundles over $\mathbb{P}^2$ or other base surfaces [12, 15–19]. The set of bases we analyze here includes those bases as special subsets, though in general the bases explored in the Monte Carlo analysis have substantially larger values of the Hodge number $h^{1,1}(B)$.

The structure of this paper is as follows: in section 2, we describe the Monte Carlo approach we use to explore threefold bases. In section 3, we give the results of our investigation, including statistics on typical base geometries and non-Higgsable clusters. Some conclusions are contained in section 4.

2   Monte Carlo on threefold bases

2.1   F-theory basics: bases and gauge groups

We review here some basic aspects of F-theory, related to the geometry of the base B and non-Abelian gauge groups associated with Kodaira singularities in the elliptic fibration. Much of the basic F-theory and relevant geometry for describing threefold bases and associated non-Higgsable clusters is described in [14] and [15], and more detail on these subjects can be found in those papers. For more general introductions to F-theory, see [11, 20, 21].

We consider four-dimensional F-theory models that come from an elliptic fibration with a section over a smooth compact toric threefold B. The total space X is a Calabi-Yau fourfold, which can be described by a Weierstrass model:

$$y^2 = x^3 + f(s,t,w)x + g(s,t,w) \tag{2.1}$$

Here we denote the local coordinates on B by complex variables s, t, w. f, g and the discriminant

$$\Delta = 4f^3 + 27g^2 \tag{2.2}$$

are sections of line bundles

$$f \in \mathcal{O}(-4K), \ g \in \mathcal{O}(-6K), \ \Delta \in \mathcal{O}(-12K), \tag{2.3}$$

where K is the canonical class of the base B. The elliptic fiber is singular at the vanishing locus of Δ. For codimension one loci on the base, the singularity types were classified by Kodaira [22]. In type IIB string theory, there are seven-branes wrapped on those loci. For different orders of vanishing for f and g, these seven-branes give rise to different non-Abelian gauge groups in the 4d supergravity theory [23–26]. We summarize the rules in table 1.

In general we expand f and g in a local coordinate w near a codimension one locus $w = 0$ as follows:

$$f = f_0 + f_1 w + f_2 w^2 + f_3 w^3 + f_4 w^4 + \dots , \ g = g_0 + g_1 w + g_2 w^2 + g_3 w^3 + g_4 w^4 + g_5 w^5 + \dots \tag{2.4}$$

The coefficients f_i, g_i are functions of the other two local coordinates s and t.

We consider only generic elliptic fibrations on B; that is, we assume that the functions f and g include all possible monomials with generic non-vanishing coefficients. The gauge groups that arise in this context are called (geometrically) non-Higgsable gauge groups. Under this condition, not all cases in table 1 are relevant in our study. The cases with ord(Δ)> 2·ord(g) are excluded. Hence the only possible non-Higgsable gauge group factors that can arise on a single divisor (up to possible discrete quotients) are SU(2), SU(3), G_2,

Type	ord (f)	ord (g)	ord (Δ)	sing.	symmetry algebra
I_0	≥ 0	≥ 0	0	none	none
I_n	0	0	$n \geq 2$	A_{n-1}	$\mathfrak{su}(n)$ or $\mathfrak{sp}(\lfloor n/2 \rfloor)$
II	≥ 1	1	2	none	none
III	1	≥ 2	3	A_1	$\mathfrak{su}(2)$
IV	≥ 2	2	4	A_2	$\mathfrak{su}(3)$ or $\mathfrak{su}(2)$
I_0^*	≥ 2	≥ 3	6	D_4	$\mathfrak{so}(8)$ or $\mathfrak{so}(7)$ or $\mathfrak{g}_2$
I_n^*	2	3	$n \geq 7$	D_{n-2}	$\mathfrak{so}(2n-4)$ or $\mathfrak{so}(2n-5)$
IV^*	≥ 3	4	8	$\mathfrak{e}_6$	$\mathfrak{e}_6$ or $\mathfrak{f}_4$
III^*	3	≥ 5	9	$\mathfrak{e}_7$	$\mathfrak{e}_7$
II^*	≥ 4	5	10	$\mathfrak{e}_8$	$\mathfrak{e}_8$
non-min	≥ 4	≥ 6	≥ 12	does not appear for SUSY vacua	

Table 1. Table of codimension one singularity types for elliptic fibrations and associated non-Abelian symmetry algebras. In cases where the algebra is not determined uniquely by the orders of vanishing of f, g, the precise gauge algebra is fixed by monodromy conditions that can be identified from the form of the Weierstrass model.

SO(7), SO(8), F_4, E_6, E_7 and E_8. There are two different kinds of non-Higgsable SU(2) gauge groups, corresponding to type III and type IV singular fibers respectively; we refer to these as SU(2)$_{III}$ and SU(2)$_{IV}$.

For the fiber types IV, I_0^* and IV^*, the gauge group is specified by additional information encoded in the "monodromy cover polynomials" $\mu(\psi)$ [24–26]. Suppose the divisor is given by a local equation $w = 0$, then for the case of type IV,

$$\mu(\psi) = \psi^2 - (g/w^2)|_{w=0} = \psi^2 - g_2. \tag{2.5}$$

When $\mu(\psi)$ can be locally factorized into

$$\mu(\psi) = (\psi + a)(\psi - a), \tag{2.6}$$

the gauge group is SU(3), otherwise it is SU(2). This means that the gauge group given by a type IV singular fiber is SU(3) if and only if g_2 is a complete square. The case of type IV^* is similar, where the monodromy cover polynomial is

$$\mu(\psi) = \psi^2 - (g/w^4)|_{w=0} = \psi^2 - g_4. \tag{2.7}$$

When g_4 is a complete square, then the corresponding gauge group is E_6, otherwise it is F_4. For the case of type I_0^*, the monodromy cover polynomial is

$$\mu(\psi) = \psi^3 + (f/w^2)|_{w=0}\psi + (g/w^3)|_{w=0} = \psi^3 + f_2\psi + g_3. \tag{2.8}$$

When $\mu(\psi)$ can be decomposed into three factors:

$$\mu(\psi) = (\psi + a)(\psi + b)(\psi - a - b), \tag{2.9}$$

the corresponding gauge group is SO(8). Otherwise if it can be decomposed into two factors:

$$\mu(\psi) = (\psi + a)(\psi^2 - a\psi + b), \tag{2.10}$$

the gauge group is SO(7). If it cannot be decomposed at all, then the gauge group is the lowest rank one: G_2.

2.2 Toric bases

To describe the geometry of the base we will use some basic language of toric geometry; see [27]. The base three-dimensional compact toric variety is described by a fan, which is a set of one, two and three dimensional cones in the integral lattice $N = \mathbb{Z}^3$. The one-dimensional cones (three-dimensional rays) $\{v_i = (v_{i,x}, v_{i,y}, v_{i,z}) \in N\}$ correspond to the toric divisors $\{D_i\}$ on the base $(i = 1, \ldots, n)$. The two-dimensional cone $v_i v_j$ corresponds to the intersection locus of the two divisors D_i and D_j, which is a toric curve. The three-dimensional cone $v_i v_j v_k$ is the intersection point of three divisors D_i, D_j and D_k. There is a universal requirement on the cones, which is that the intersection of any of those cones is also a cone (or $\varnothing$). Hence, any toric curve $v_i v_j$ is contained in exactly two three-dimensional cones: $v_i v_j v_k$ and $v_i v_j v_l$. The essential information about a toric threefold B is then the set of toric divisors $\{D_i\}$ and the set of three-dimensional cones $\{\sigma_p = v_i v_j v_k\}$. Furthermore, the total number of three-dimensional cones is fixed to be $|\{\sigma_p\}| = 2n - 4$. For a smooth variety, it is required that the three-dimensional cones have unit volume: for all $\sigma_p = v_i v_j v_k$, $|(v_i \times v_j) \cdot v_k| = 1$.

Actually, the toric divisors $\{D_i\}$ are not entirely linearly independent in homology. There are three linear relations:

$$\sum_{i=1}^{n} v_{i,x} D_i = 0, \quad \sum_{i=1}^{n} v_{i,y} D_i = 0, \quad \sum_{i=1}^{n} v_{i,z} D_i = 0. \tag{2.11}$$

Hence the rank of the Picard group of B is rk(Pic(B))= $h^{1,1}(B) = n - 3$.

The canonical class K of the base B is given by

$$K = -\sum_{i=1}^{n} D_i. \tag{2.12}$$

On B we can define the triple intersection numbers $D_i \cdot D_j \cdot D_k$. For $i \neq j \neq k$, if v_i, v_j, v_k are in a three-dimensional cone σ_p, then $D_i \cdot D_j \cdot D_k = 1$. Otherwise it is zero. All the triple intersection numbers involving self products can be determined by the linear relations (2.11) and the fact that $D_i \cdot D_j \cdot D_k$ vanishes if $D_i D_j (i \neq j)$ is not a toric curve (Actually those $D_i D_j$ generate the Stanley-Reisner ideal of B). However, unlike the case of 2d toric bases, those triple intersection numbers do not seem to provide a simple direct approach to the classification of non-Higgsable clusters.

Two toric bases B_1 and B_2 are equivalent if their defining rays are related by a lattice isomorphism of $N = \mathbb{Z}^3$, while keeping the set of cones $\{\sigma_p\}$ unchanged.

2.3 Blow-ups and blow-downs

To move between different threefold bases, we can use blow-ups or blow-downs to increase or decrease the rank of the Picard group. There are two kinds of blow up operations on toric bases B: one can either blow up a point that corresponds to a three-dimensional
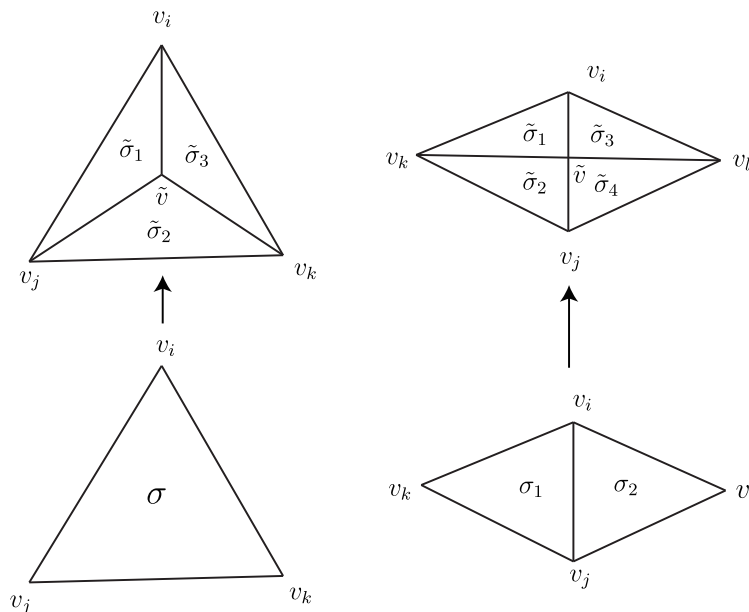
Figure 1. Illustration of two different kinds of blow ups, viewed from above. The left case corresponds to blowing up a point $v_i v_j v_k$. The right case corresponds to blowing up a curve $v_i v_j$.

cone $\sigma = v_i v_j v_k$ or blow up a toric curve $v_i v_j$, see figure 1. In the first case, a new ray $\tilde{v} = v_i + v_j + v_k$ is introduced. The old three-dimensional cone σ is removed, and three new three-dimensional cones $\tilde{\sigma}_1 = v_i v_j \tilde{v}$, $\tilde{\sigma}_2 = v_j v_k \tilde{v}$, $\tilde{\sigma}_3 = v_k v_i \tilde{v}$ are included. For the second case, a new ray $\tilde{v} = v_i + v_j$ is introduced. Suppose that there are two old 3d cones $\sigma_1 = v_i v_j v_k$ and $\sigma_2 = v_i v_j v_l$ that contain the toric curve $v_i v_j$. They are removed after the blow up. Four new 3d cones $\tilde{\sigma}_1 = v_i v_k \tilde{v}$, $\tilde{\sigma}_2 = v_j v_k \tilde{v}$, $\tilde{\sigma}_3 = v_i v_l \tilde{v}$, $\tilde{\sigma}_4 = v_j v_l \tilde{v}$ are included. Note that $v_i v_j$ is no longer a toric curve after the blow up. Similarly a blow down is defined to be the inverse process of a blow up (or as the contraction of a ray). Given a ray v, it may or may not be contracted depending on the neighboring rays. If there are only 3 neighboring rays v_i, v_j, v_k and they satisfy $v = v_i + v_j + v_k$, then v can be contracted into a point. If there are 4 neighboring rays v_i, v_k, v_j, v_l (in cyclic order around the curve), if $v = v_i + v_j$ or $v = v_k + v_l$, then v can be contracted into toric curve $v_i v_j$ or $v_k v_l$ respectively. For all the other cases, the ray v cannot be contracted.

When there are rays v_i, v_j, v_k, v_l that satisfy the relation $v_i + v_j = v_k + v_l$, and there is a 2d cone $v_i v_j$, then there exists a "flop" operation, which is a combination of a blow up and a blow down; see figure 2.

By starting with one toric base, which we take in this work to be $\mathbb{P}^3$, and performing successive blow-ups and blow-downs, we can explore a large range of threefold bases that are connected through these transitions. We restrict attention to bases that support elliptic Calabi-Yau fourfolds and associated F-theory models without tensionless strings, as determined by the criterion that there are no codimension 1 or 2 loci where f, g, Δ vanish to orders $(4, 6, 12)$. The precise formulation of this condition for toric threefold bases is discussed further in section 2.4. While there are allowed toric bases that cannot be reached
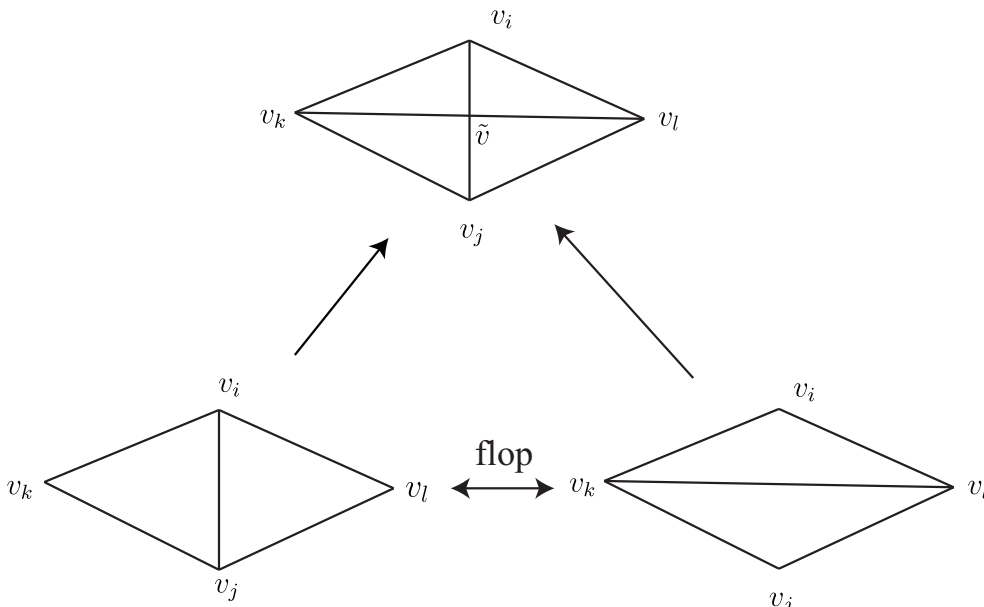
Figure 2. Illustration of the flop process, which can happen when $v_i + v_j = v_k + v_l$.

from $\mathbb{P}^3$ in this way, the set of bases that are connected to $\mathbb{P}^3$ by a sequence of single blow-up or blow-down transitions form a large class of bases; these are the object of study in this work. For 2d base surfaces, it is known that all allowed toric bases are connected through blow-up and blow-down transitions [6] to the minimal model bases given by $\mathbb{P}^2$ and the Hirzebruch surfaces [28, 29]; to get to certain bases (such as, e.g., $\mathbb{F}_{12}$) from a starting point such as $\mathbb{P}^2$, however, requires passing through intermediate bases that contain points (codimension two loci) where f, g vanish to orders $(4, 6)$, corresponding to tensionless strings and superconformal sectors [3, 30–33]; blowing up these points gives a transition to a base with an additional tensor multiplet and larger $h^{1,1}$. We do not include bases containing such codimension two loci in our study; as in the 6d (complex surface base) case this means that certain toric threefold bases will be disconnected from the set under study. Furthermore, the analogue (described using Mori theory [34]) of the minimal base surfaces for threefold bases is not known explicitly, and there is no proof that all threefold bases that support elliptic Calabi-Yau threefolds are connected through simple geometric transitions. Nonetheless, the class of bases that we study here, which are connected to $\mathbb{P}^3$ by a sequence of allowed blow-up or blow-down transitions through allowed bases that have no codimension two $(4, 6)$ loci, seem to form a large and sufficiently diverse class of bases to give interesting information about a fairly generic class of threefold F-theory bases.

2.4 Toric monomials and non-Higgsable clusters

The origin $(0, 0, 0) \in N$ represents a complex torus $(\mathbb{C}^*)^3$, which has three coordinates S, T, W. The sets of holomorphic monomials that are sections of specific line bundles on B are subsets of the dual integral lattice $M = \text{Hom}(N, \mathbb{Z})$. The monomial $S^a T^b W^c$ is represented by $(a, b, c) \in M$. Each of the three-dimensional cones $\sigma = v_i v_j v_k$ represents a

local coordinate patch. Over this patch the ring of holomorphic monomials is described by the dual cone

$$\sigma^* = \{u \in M | \langle u, v_i \rangle \geq 0 \,, \ \langle u, v_j \rangle \geq 0 \,, \ \langle u, v_k \rangle \geq 0\}. \tag{2.13}$$

Using this information we can write down the local coordinates in that patch and the transition rules between different patches. If the three divisors D_i, D_j and D_k are given by local equations $w = 0$, $s = 0$ and $t = 0$, then the monomial $u \in M$ corresponds to $w^{\langle u, v_i \rangle} s^{\langle u, v_j \rangle} t^{\langle u, v_k \rangle}$.

Now we can construct the set of monomials appearing in f, g and Δ. We denote them by $\{f\}$, $\{g\}$ and $\{\Delta\}$. They are given by:

$$\begin{aligned}
\{f\} &= \{u \in M | \forall v_i \,, \ \langle u, v_i \rangle \geq -4\}, \\
\{g\} &= \{u \in M | \forall v_i \,, \ \langle u, v_i \rangle \geq -6\}, \\
\{\Delta\} &= \{u \in M | \forall v_i \,, \ \langle u, v_i \rangle \geq -12\}.
\end{aligned} \tag{2.14}$$

The order of vanishing of f, g and Δ on a toric divisor D_i is then

$$\begin{aligned}
\mathrm{ord}_{D_i}(f) &= \min(\langle u, v_i \rangle + 4)|_{u \in \{f\}}, \\
\mathrm{ord}_{D_i}(g) &= \min(\langle u, v_i \rangle + 6)|_{u \in \{g\}}, \\
\mathrm{ord}_{D_i}(\Delta) &= \min(\langle u, v_i \rangle + 12)|_{u \in \{\Delta\}}.
\end{aligned} \tag{2.15}$$

We can also write down the order of vanishing of f, g and Δ on a toric curve $D_i D_j$:

$$\begin{aligned}
\mathrm{ord}_{D_i D_j}(f) &= \min(\langle u, v_i \rangle + \langle u, v_j \rangle + 8)|_{u \in \{f\}}, \\
\mathrm{ord}_{D_i D_j}(g) &= \min(\langle u, v_i \rangle + \langle u, v_j \rangle + 12)|_{u \in \{g\}}, \\
\mathrm{ord}_{D_i D_j}(\Delta) &= \min(\langle u, v_i \rangle + \langle u, v_j \rangle + 24)|_{u \in \{\Delta\}}.
\end{aligned} \tag{2.16}$$

$\mathrm{ord}_{D_i D_j}(f, g, \Delta)$ can be greater or equal to $\mathrm{ord}_{D_i}(f, g, \Delta) + \mathrm{ord}_{D_j}(f, g, \Delta)$. This is different from the case of 2d bases, where the order of vanishing on the intersection point of two divisors is always the sum of the orders of vanishing on those two divisors.

Similarly we can write down the order of vanishing of f, g and Δ on the point $D_i D_j D_k$:

$$\begin{aligned}
\mathrm{ord}_{D_i D_j D_k}(f) &= \min(\langle u, v_i \rangle + \langle u, v_j \rangle + \langle u, v_k \rangle + 12)|_{u \in \{f\}}, \\
\mathrm{ord}_{D_i D_j D_k}(g) &= \min(\langle u, v_i \rangle + \langle u, v_j \rangle + \langle u, v_k \rangle + 18)|_{u \in \{g\}}, \\
\mathrm{ord}_{D_i D_j D_k}(\Delta) &= \min(\langle u, v_i \rangle + \langle u, v_j \rangle + \langle u, v_k \rangle + 36)|_{u \in \{\Delta\}}.
\end{aligned} \tag{2.17}$$

For a good F-theory base, we exclude the cases where the order of vanishing of f and g reaches 4 and 6 on a divisor:

$$\mathrm{ord}_{D_i}(f) \geq 4 \,, \ \mathrm{ord}_{D_i}(g) \geq 6 \ \Rightarrow \ \text{excluded} \tag{2.18}$$

or on a curve:

$$\mathrm{ord}_{D_i D_j}(f) \geq 4 \,, \ \mathrm{ord}_{D_i D_j}(g) \geq 6 \ \Rightarrow \ \text{excluded} \tag{2.19}$$

As mentioned above, in the case of a curve a $(4, 6)$ locus indicates the appearance of a tensionless string, so that the low-energy theory does not have a conventional field theory

description; such curves can be blown up to get another base that generally supports a less singular elliptic CY threefold. We also exclude the bases where the order of vanishing of f and g reaches 8 and 12 on a toric intersection point:[1]

$$\text{ord}_{D_i D_j D_k}(f) \geq 8, \quad \text{ord}_{D_i D_j D_k}(g) \geq 12 \Rightarrow \text{excluded} \tag{2.20}$$

Practically, since the elliptic fibration is generic we only need to check the order of vanishing for g.

Apart from the constraints (2.18)–(2.20), there are also other cases where $\text{ord}_{D_i}(f) \geq 4$, $\text{ord}_{D_i}(g) = 5$, but the expansion coefficient g_5 in (2.4) contains more than one monomial. When this happens, g_5 is not constant, which means that there is a locus $\Sigma \in D_i$ such that $\text{ord}_\Sigma(g) = 6$. This type of $(4, 6)$ singularity on a curve is analogous to that which arises at points on the (-9), (-10), (-11)-curves on 2d bases [5]. We exclude toric bases with such $(4, 6)$ curves, though they may admit blow-ups to non-toric bases that support good F-theory compactifications.

Using the information of $\{f\}$ and $\{g\}$, we can read off the non-Higgsable gauge group on each divisor. We explicitly describe the rules for non-Higgsable type IV, IV^* and I_0^* singularities; see also [12, 14].

When $\text{ord}_{D_i}(f) \geq 2$, $\text{ord}_{D_i}(g) = 2$, the singularity type is IV. In this case when g_2 only contains one monomial $u \in M$, and furthermore $u \in 2M$ is even and therefore a perfect square, then the gauge group is SU(3). Otherwise the gauge group is type SU(2)$_{IV}$.

When $\text{ord}_{D_i}(f) \geq 3$, $\text{ord}_{D_i}(g) = 4$, the singularity type is IV^*. In this case when g_4 only contains one monomial $u \in M$, and furthermore $u \in 2M$, then the gauge group is E_6. Otherwise the gauge group is F_4.

When $\text{ord}_{D_i}(f) \geq 2$, $\text{ord}_{D_i}(g) = 3$ or $\text{ord}_{D_i}(f) = 2$, $\text{ord}_{D_i}(g) > 3$, the singularity type is I_0^*. When the monodromy cover polynomial (2.8) can be written as

$$\mu(\psi) = \psi^3 + f_2 \psi + g_3 = \psi^3 - (a^2 - b)\psi + ab, \tag{2.21}$$

the gauge group is SO(7) or SO(8). The gauge group is SO(8) only when $\mu(\psi)$ can be written as

$$\mu(\psi) = \psi^3 + f_2 \psi + g_3 = \psi^3 - (a^2 + ab + b^2)\psi - (a + b)ab. \tag{2.22}$$

Now if $\text{ord}_{D_i}(f) = 2$ and $\text{ord}_{D_i}(g) > 3$, $\mu(\psi) = \psi^3 + f_2\psi$, the gauge group is either SO(7) or SO(8). The gauge group is SO(8) only when $a = 0$ or $b = 0$ or $a + b = 0$ in (2.22). Then it is required that f_2 only contains one monomial $u \in M$, and furthermore $u \in 2M$. Otherwise the gauge group is SO(7).

For the other case, $\text{ord}_{D_i}(f) \geq 2$ and $\text{ord}_{D_i}(g) = 3$, for generic f, g, μ can only have the form (2.21) if f_2 and g_3 each contain only single monomials and $b \sim a^2$. This can be seen by simply considering the number of independent monomials in a, b compared to f_2, g_3. Thus, when $f_2 \sim a^2$ and $g_3 \sim a^3$ for a single monomial a, $\mu(\psi)$ can be written in form of (2.22) and the gauge group is SO(8); otherwise the gauge group is G_2.

---

[1]It is not clear whether it is problematic or not when the orders of vanishing of f and g reach (4,6) at a codimension-three locus [35]. Here, as in [14], we use the weaker condition (2.20).

2.5 Fourfold geometry

Much of the relevant geometry of the generic elliptic Calabi-Yau fourfold fibered over the threefold base B can be read off directly from the geometry of B.

From the full non-Abelian non-Higgsable gauge group G, we can compute the Hodge number $h^{1,1}(X)$ of the Calabi-Yau fourfold, using the Shioda-Tate-Wazir formula [3, 36]

$$h^{1,1}(X) \cong \tilde{h}^{1,1}(X) = h^{1,1}(B) + \mathrm{rk}(G) + 1. \tag{2.23}$$

Here we assume that there is no non-Higgsable U(1) gauge group. For all the 2d toric bases, such contributions to $h^{1,1}(X_3)$ never appear [6], though we do not know for sure that this cannot happen for toric 3d bases.

We can also compute the Hodge number $h^{3,1}(X)$, using an approximate Batyrev type formula [37]:

$$h^{3,1}(X) \cong \tilde{h}^{3,1}(X) \tag{2.24}$$
$$= |\{f\}| + |\{g\}| - \sum_{\Theta \in \Delta, \dim \Theta = 2} l'(\Theta) - 4 + \sum_{\Theta_i \in \Delta, \Theta_i^* \in \Delta^*, \dim(\Theta_i) = \dim(\Theta_i^*) = 1} l'(\Theta_i) \cdot l'(\Theta_i^*).$$

Here Δ^* is the convex hull of $\{v_i\}$ and Δ is the dual polytope of Δ^*, defined to be

$$\Delta = \{u \in \mathbb{R}^3 | \forall v \in \Delta^*, \ \langle u, v \rangle \geq -1\}. \tag{2.25}$$

The symbol Θ denotes 2d faces of Δ. Θ_i and Θ_i^* denote the 1d edges of the polytopes Δ and Δ^*. $l'(\cdot)$ counts the number of integral interior points on a face. While this formula is only proven for a subclass of toric threefold bases, and may be off by small amounts for some choices of B, we expect that it is a good approximate measure of $h^{3,1}(X)$.

Because both formulae used here are not rigorously proven for all toric threefold bases, and we only use them as approximate measures of the Hodge numbers, we have used tildes to denote the approximate Hodge numbers $\tilde{h}^{1,1}, \tilde{h}^{3,1}$ given by these formulae.

2.6 Random walks on the connected set of toric threefold bases

In order to characterize generic properties of a 3d toric base in 4d F-theory, we can perform a random walk from some starting point, say $\mathbb{P}^3$. In each step of the random walk, the base may be blown up or blown down to get another acceptable base. Depending upon the weighting of the probabilities of each move, we get a specific resulting distribution on the set $\mathcal{C}$ of connected valid 3d toric bases without $(4, 6)$ curves.

We perform the random walk using an equal weighting for each valid blow-up or blow-down from a given base $B \in \mathcal{C}$. It is easy to see that a random walk on a graph where each node V_i has n_i neighbors, where neighbors are chosen uniformly on each step of the walk, will give a distribution on nodes proportional to n_i, since the probability of traversing each link in either direction is then equal. A potential obstruction to using this algorithm in the case at hand is the computational burden of determining which neighbors are valid; for a toric threefold base having a fan with n rays and $h^{1,1}(B) = n - 3$, the number of faces (three-dimensional cones) is $2n - 4$, and the number of edges (two-dimensional cones)

is is $3n - 6$, so the number of possible moves goes as $6n$. For $n \sim 100$, this makes it very costly to evaluate all possible blow-ups and blow-downs for validity. Thus, we use a simpler algorithm of simply choosing a possible blow-up or blow-down at random from the set of all the $6n - 10$ possible 3d cones, 2d cones, and rays, and then testing the chosen move to see if it results in an allowed base. If the tested step does not lead to an allowed base, we try again. This effectively gives a random walk where all allowed moves are weighted equally, so that over a large number of steps we expect a "thermal" distribution in which the probability of each base B in the set $\mathcal{C}$ connected to the starting base $\mathbb{P}^3$ is proportional to n_i, the number of valid neighbors to which B is connected by single blow-up or blow-down moves. To get a uniform distribution on the set of allowed bases we need to weight our statistics by the factor $1/n_i$ for each base. Because we do not explicitly compute n_i for the reasons given above, we estimate the weighting factor in a crude way by computing the number t of tries needed to identify an allowed neighbor. Naively the number of allowed neighbors of a given base B should then be $(6n - 10)/\langle t \rangle$, where $\langle t \rangle$ is the average number of tries needed to identify an allowed neighbor over many trials on the base B. The weighting factor $1/n_i$ can therefore be estimated as $\langle t \rangle/(6n - 10)$, so we can estimate quantities statistically by weighting each base with the factor $t/(6n - 10)$.

Sometimes, however, the different neighbors of one base can be equivalent. For example, consider a graph with only three nodes: $\mathbb{P}^3$, $\mathrm{blp}_{\mathrm{cone}}\mathbb{P}^3$ and $\mathrm{blp}_{\mathrm{curve}}\mathbb{P}^3$. $\mathrm{blp}_{\mathrm{cone}}\mathbb{P}^3$ and $\mathrm{blp}_{\mathrm{curve}}\mathbb{P}^3$ denote the bases that result from blowing up a (3d) cone or a curve on $\mathbb{P}^3$ respectively. We explicitly list the rays and 3d cones for these three toric threefold bases below:

$$\mathbb{P}^3 \quad : \quad v_1 = (1, 0, 0), v_2 = (0, 1, 0), v_3 = (0, 0, 1), v_4 = (-1, -1, -1),$$
$$\{\sigma_p\} = \{v_1 v_2 v_3, v_1 v_2 v_4, v_1 v_3 v_4, v_2 v_3 v_4\} \tag{2.26}$$

$$\mathrm{blp}_{\mathrm{cone}}\mathbb{P}^3 \quad : \quad v_1 = (1, 0, 0), v_2 = (0, 1, 0), v_3 = (0, 0, 1), v_4 = (-1, -1, -1), v_5 = (1, 1, 1),$$
$$\{\sigma_p\} = \{v_1 v_2 v_4, v_1 v_3 v_4, v_2 v_3 v_4, v_1 v_2 v_5, v_1 v_3 v_5, v_2 v_3 v_5\} \tag{2.27}$$

$$\mathrm{blp}_{\mathrm{curve}}\mathbb{P}^3 \quad : \quad v_1 = (1, 0, 0), v_2 = (0, 1, 0), v_3 = (0, 0, 1), v_4 = (-1, -1, -1), v_5 = (1, 1, 0),$$
$$\{\sigma_p\} = \{v_1 v_3 v_4, v_2 v_3 v_4, v_1 v_3 v_5, v_1 v_4 v_5, v_2 v_3 v_5, v_2 v_4 v_5\} \tag{2.28}$$

There are four ways to get $\mathrm{blp}_{\mathrm{cone}}\mathbb{P}^3$ and six ways to get $\mathrm{blp}_{\mathrm{curve}}\mathbb{P}^3$ from blowing up a cone or curve on $\mathbb{P}^3$, since there are 4 3d-cones and 6 2d-cones in the toric fan of $\mathbb{P}^3$. This means that naively $\mathbb{P}^3$ has 10 neighbors, and the base is weighted by $1/10$. Now, if we perform a random walk on this graph, the expected probability ratio is $p(\mathbb{P}^3)$: $p(\mathrm{blp}_{\mathrm{cone}}\mathbb{P}^3)$: $p(\mathrm{blp}_{\mathrm{curve}}\mathbb{P}^3) = 10 : 4 : 6$. Then after we weight $p(\mathbb{P}^3)$ by a factor $1/10$, the expected probability ratio becomes $1 : 4 : 6$, which is still far from uniform. To fix this problem we compute the symmetry factor F of each base, which is defined to be the order of the subgroup of the permutation group acting on the toric divisors of the base that preserves the cone structure. For example, for the base $\mathbb{P}^3$, since all the four rays v_1, v_2, v_3, v_4 can be permuted arbitrarily without changing the cone structure, $F(\mathbb{P}^3) = 24$. For the base $\mathrm{blp}_{\mathrm{cone}}\mathbb{P}^3$, the divisors corresponding to v_1, v_2 and v_3 can be permuted, hence $F(\mathrm{blp}_{\mathrm{cone}}\mathbb{P}^3) = 6$. For the base $\mathrm{blp}_{\mathrm{curve}}\mathbb{P}^3$, there are two symmetric divisor pairs: (v_1, v_2)

and (v_3, v_4), hence $F(\text{blp}_{\text{curve}}\mathbb{P}^3) = 4$. After we multiply those symmetry factors by the ratio $1 : 4 : 6$, then we achieve a uniform distribution. In general, if there are m ways to get equivalent bases B from k equivalent bases A with symmetry factor $F(A)$, then the symmetry factor of B satisfies $mF(B) = kF(A)$. Hence this inclusion of symmetry factors solves the problem.

For a general base with a large number of rays, the probability of having a nontrivial symmetry is negligible. So practically, the inclusion of symmetry factors only affects the statistics of bases with a number of rays $n \lesssim 10$.

In the following section we present results of this Monte Carlo approach.

3 Results

3.1 Choices of Monte Carlo parameters

Our primary analysis was carried out by doing 100 independent runs of 100,000 bases, each starting at $\mathbb{P}^3$ and exploring a subset of the bases in the connected set $\mathcal{C}$ using a random walk as described above. In the remaining parts of this paper we refer to these 100 runs as "unbounded" runs, to distinguish them from other runs (with bounded $h^{1,1}(B)$) described in section 3.2.2. The first 500 or so bases in each unbounded run had atypically small values of $h^{1,1}(B)$. We compute our statistics based on the subset after each run has approximately thermalized, by dropping the first 1000 bases. As we discuss further in the following sections, each run rapidly seems to have entered a local region, or *domain*, of the allowed space of bases that may only be connected to the other domains through relatively rare paths in the graph that may require an excursion to relatively low $h^{1,1}$. Thus, it seems that these individual runs are not truly thermalized in a global sense. Nonetheless, the distributions in each domain are sufficiently similar and regularly distributed between domains that we take the set of data from the 100 independent runs as presumably relatively representative of the full set $\mathcal{C}$ of connected bases. Further more extensive analysis would be necessary to rigorously demonstrate or counter this hypothesis. We also note in parts of the analysis some distinctions between the different domains explored by the independent runs.

3.2 Distribution and number of threefold bases

3.2.1 Distribution of bases

We begin by considering the distribution of bases as estimated by the Monte Carlo analysis using some fairly simple measures.

As described in section 2.6, we estimate the proper weighting factor for each base B encountered by $t \cdot F(B)/(6n - 10)$, where n is the number of rays for the fan of B, t is the number of tries needed to find an allowed neighbor, and $F(B)$ is the symmetry factor of B.

The total distribution is graphed in figure 3 and compared to the distributions for several individual runs.

From the distinct shapes of the distributions from individual runs, we see evidence for the observation mentioned above that each run is probing a different domain in the connected space of bases. One particular run, for example, probed a set of bases with
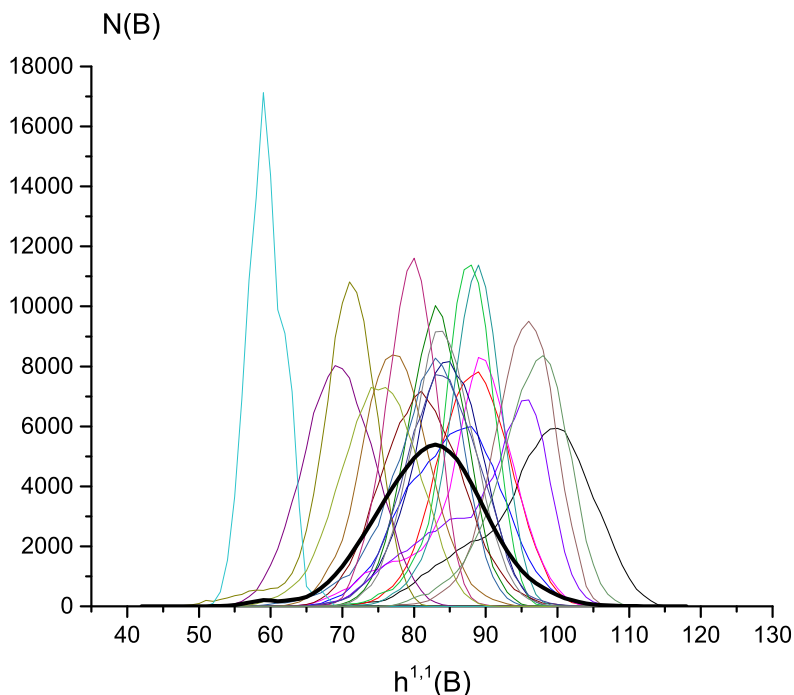
Figure 3. The distribution of $h^{1,1}(B)$, including weighting factors. Bold black curve is total distribution (divided by the number of runs, 100), colored curves are some example distributions from individual runs. The total number of samples in each run is normalized to 100,000.

anomalously low $h^{1,1}(B)$ values, giving rise to the small bump on the left tail of the total distribution shown in figure 3. A much longer (perhaps impossibly long in practice) Monte Carlo run would be needed to have true thermalization between the domains in a single run.

The overall mean and standard deviation of $h^{1,1}(B)$ are

$$\langle h^{1,1}(B) \rangle = 82 \tag{3.1}$$

$$\sigma(h^{1,1}(B)) = 6. \tag{3.2}$$

Comparing the distinct runs, the mean value in each run ranged from 59.4 to 96.8, with a standard deviation of 6.

As mentioned in the introduction, simple bases such as toric Fano threefolds, $\mathbb{P}^1$ bundles over $\mathbb{P}^2$ and $\mathbb{P}^2$ bundles over $\mathbb{P}^1$, as studied in [16–18], have very small values of $h^{1,1}(B)$, and are only encountered in the first stages of the Monte Carlo runs, before thermalization. Larger classes of $\mathbb{P}^1$ bundles over more general base surfaces were explored in [12] and [15]. In particular, in [15], the full set of threefolds that have the form of $\mathbb{P}^1$ bundles over toric surfaces S that themselves support elliptic Calabi-Yau threefolds was explored. That set included threefolds with a larger range of values of $h^{1,1}(B)$, and is more closely analogous to the distribution of bases studied here. As we mention again below, the qualitative distribution of physical features on that set is roughly compatible with what we have found in the Monte Carlo analysis, although the $\mathbb{P}^1$-bundle threefolds have certain characteristic features that affect the distribution of e.g. non-Higgsable clusters that arise on those bases.
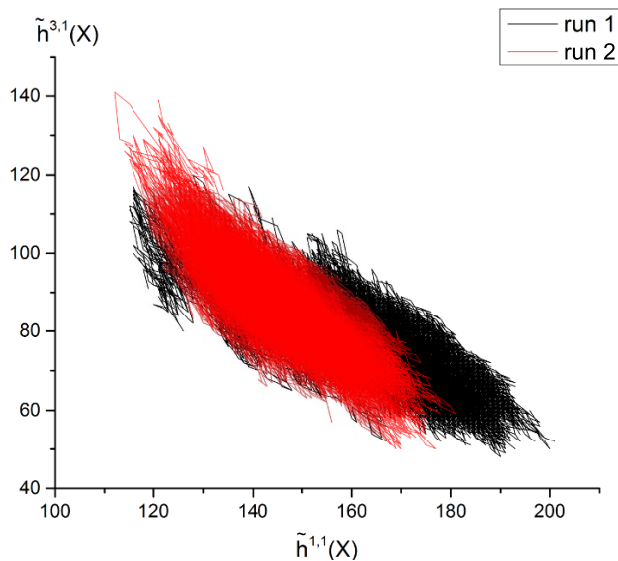
Figure 4. (Approximate) Hodge numbers for generic elliptically fibered fourfolds over the bases B encountered in two of the random walks through the space of connected bases.
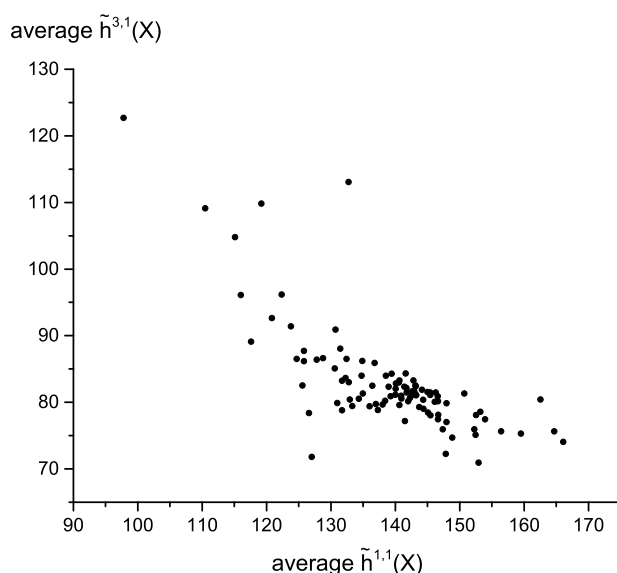

Figure 5. Mean values of the (approximate) Hodge numbers for generic elliptic Calabi-Yau fourfolds over the threefold bases encountered in each of the independent Monte Carlo runs.

It is helpful to get a sense of how each run explores the space of possible bases by graphing the set of (approximate) Hodge numbers $\tilde{h}^{1,1}(X), \tilde{h}^{3,1}(X)$ of the generic elliptically fibered Calabi-Yau fourfolds over the sets of bases B explored by the separate runs. Two sample runs are shown in figure 4. The mean Hodge numbers across each run are shown in figure 5. These Hodge numbers can be compared to the distribution of Hodge numbers known for general Calabi-Yau fourfolds constructed using toric and related methods [16, 38, 39], as depicted in figure 6.
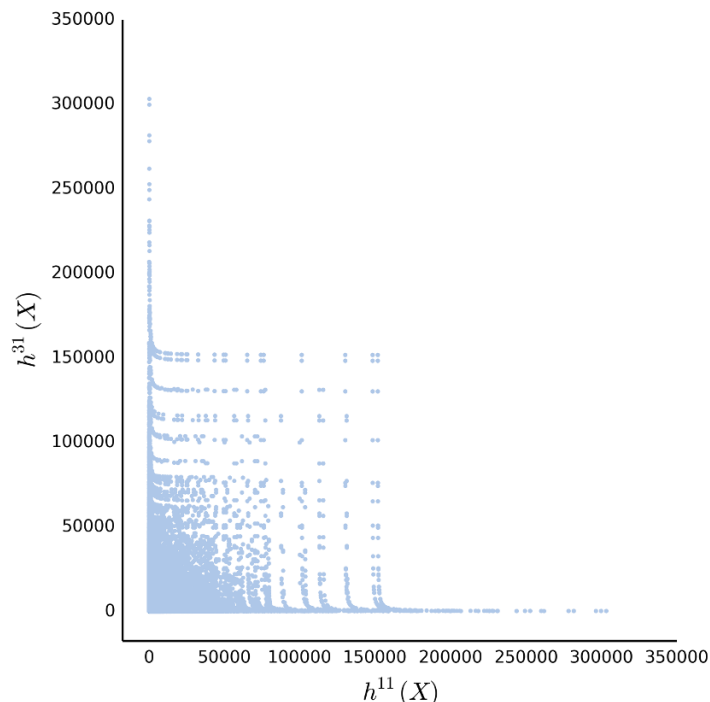
Figure 6. Distribution of Hodge numbers for Calabi-Yau fourfolds constructed as hypersurfaces in weighted projective space using reflexive polytopes [39].

Though the fourfolds we encounter in the Monte Carlo exploration have relatively small Hodge numbers compared to the limits realized in the full set of known Calabi-Yau fourfolds, the Hodge numbers are clustered in a region that is not far from the peak of the distribution in the set of known fourfolds, at least for those that arise from reflexive transverse weight systems. Figure 7 compares the distribution of $h^{1,1} + h^{3,1}$ encountered in the Monte Carlo runs to the distribution found for a particular set of fourfold constructions, namely the transverse weight systems found in [38] that give reflexive polytopes. Note that the Monte Carlo distribution is much more peaked than that for the known fourfolds. There are several possible reasons for this. First, bases with small $h^{1,1}(B)$ can support a wide range of "tunings" of the Weierstrass model corresponding to distinct codimension one and two singularity structures giving distinct Calabi-Yau fourfolds with relatively small Hodge numbers over the same base, while bases giving elliptic Calabi-Yau's with larger Hodge numbers admit fewer tunings (see e.g. [9]). This in general increases the number of fourfolds at small Hodge numbers disproportionately to the number of bases. The fourfolds that do not admit elliptic fibrations with section may also be more common at smaller Hodge numbers. At larger Hodge numbers, there are fourfolds that support non-Higgsable E_8 factors that arise from toric constructions with $(4, 6)$ curves, which are not included in this analysis. These may increase the number of fourfolds with higher Hodge numbers relative to the distribution of bases found in the Monte Carlo. Finally, there can be many weight systems that give rise to the same Calabi-Yau, which may artificially enhance the distribution of weight systems in certain regimes. These issues make the

– 15 –

comparison in figure 7 a rather rough analogy, but the rough agreement between the regions of the peak suggests that with the preceding caveats, somewhat similar distributions may be sampled by the two different approaches. To get a sense of the significance of this comparison, we have considered a similar analysis in the case of elliptic threefolds, with results shown in figure 8. In that graph we compare the set of Hodge numbers for an analogous class of weight systems that give known Calabi-Yau threefolds from hypersurfaces in toric varieties [41–43] (data available at [40][2]) to generic elliptic fibrations over the full set of toric base surfaces that support elliptic Calabi-Yau threefolds (identified in [6]) and the subset in the connected set $\mathcal{C}_3$ related to $\mathbb{P}^2$ by blow-ups and blow-downs that do not introduce $(4, 6)$ points. In the 3D case we see that the connected set has a similar shape but somewhat smaller size and lower Hodge numbers from the complete set of toric bases. And we see a similar rough agreement between the peaks of the distributions, which are all well below the largest possible Hodge numbers realized for threefolds. As in the fourfold case, the distribution from the connected set of base surfaces is more peaked and undercounts the number of threefolds at both small and large Hodge numbers. In the case of threefolds explicit consideration of the distributions shows that the reasons given above seem to characterize the differences between the distributions accurately. Note in particular that there are many distinct weight systems that can characterize the same reflexive polytope and elliptic threefold; this explains the excess in the graph of the distribution of weight systems compared to toric bases at large Hodge numbers seen in figure 8. In fact, at very large Hodge numbers all known threefolds are elliptic fibrations over toric bases, with little tuning possible.

Analyses from several points of view [7, 9, 42, 44–46] suggest that in fact most or all known Calabi-Yau threefolds and fourfolds with large Hodge numbers admit an elliptic fibration. Thus, both for threefolds and for fourfolds we may expect that a complete analysis of the bases involved, including tunings of the generic Weierstrass model, may give a good picture of the set of possible elliptic Calabi-Yau manifolds. In any case, the rough similarity between figure 7 and the fairly parallel 3d analysis depicted in figure 8 suggests that the Monte Carlo analysis of threefold bases is exploring a reasonably representative sample of the bases associated with a significant part of the space of known fourfolds. As in the case of threefold bases, we expect that our Monte Carlo is missing an even larger number of bases that have $(4, 6)$ curves, associated with non-toric threefolds that support Calabi-Yau fourfolds giving F-theory models with E_8 gauge factors. It would be nice to extend the kind of analysis we do in this paper to include these other bases, though this is technically more complicated than in the simpler case of base surfaces for elliptic threefolds.

3.2.2 The number of threefold bases

The number of bases in the connected set we are exploring appears to be quite large. In particular, the tendency of the Monte Carlo runs to enter separated domains in the graph of connected bases indicates that the total number of bases available is at least much larger than 10^5. The individual Monte Carlo runs we have carried out generally do not

---

[2]Kreuzer and Skarke have made a large database of information on Calabi-Yau threefolds and fourfolds available online.
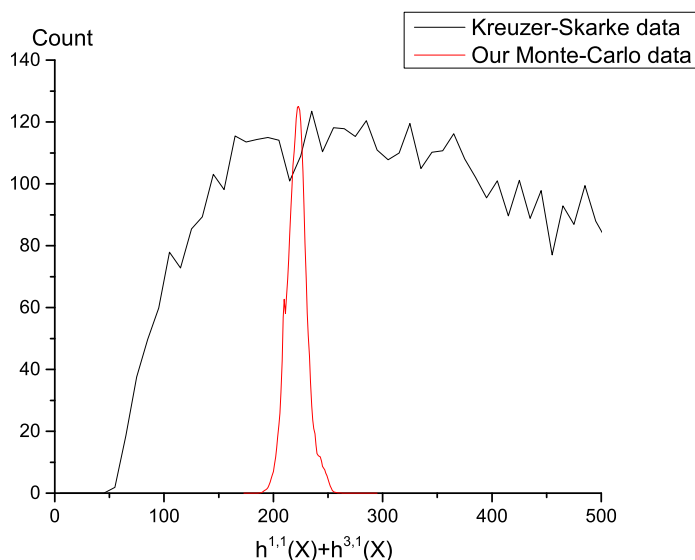
Figure 7. The weighted distribution of bases found in the Monte Carlo as a function of $\tilde{h}^{1,1}(X) + \tilde{h}^{3,1}(X)$, compared to the set of fourfolds identified in [38], as hypersurfaces in 5d reflexive polytopes corresponding to transverse weight systems. The scale on the Monte Carlo data is not significant and is chosen based on the size of the Monte Carlo runs, which happens to give it a compatible scale for easy comparison with the fourfold data (available from [40]).
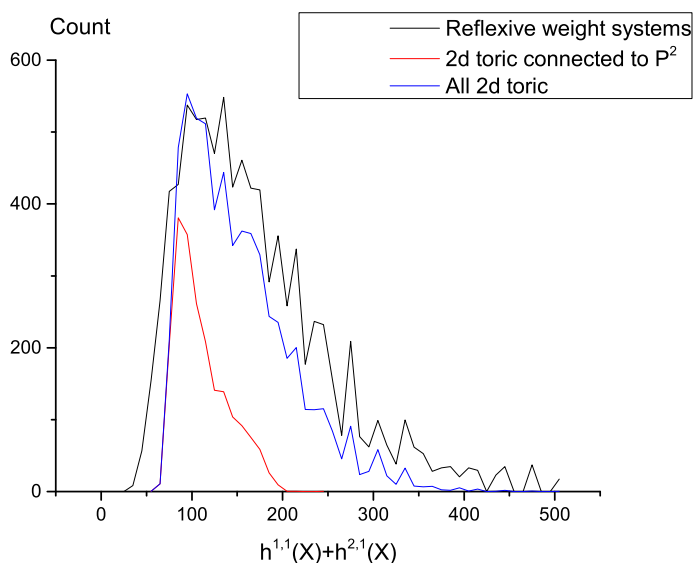

Figure 8. Comparison of the distribution of Hodge numbers in the known Kreuzer-Skarke Calabi-Yau threefold database with the set of Hodge numbers for generic elliptically fibered CY threefolds over both the full set of toric bases [6] and the subset in the connected set $\mathcal{C}_3$ related to $\mathbb{P}^2$ by blow-ups and blow-downs that do not introduce $(4,6)$ points. In order to match up with figure 7, we only choose the subset in the Kreuzer-Skarke database that corresponds to reflexive weight systems [41].

hit bases with $h^{1,1}(B) \lesssim 50$ once they have "thermalized" after 1000 or more steps. To get a normalization on the distribution and thus estimate the total number of bases, we have carried out a sequence of runs in which we have placed an artificial upper bound on the Picard number of the base. In particular, we have done 10 Monte Carlo runs of 30,000 steps each with upper bounds $h^{1,1}(B) \leq 5k + 2$ for each $k = 1, \ldots, 13$. We again ignore the first 1000 bases in all the statistical analyses. Using the appropriate weighting factors, this gives an estimate of the distribution of bases in each bounded range of $h^{1,1}(B)$.

The (logarithmically scaled) distributions of bases for the first few values of k are shown in figure 9.

To estimate the total number of bases in $\mathcal{C}$ we can combine the distributions from the bounded runs. We define

$$N(h) = |\{B \in \mathcal{C} : h^{1,1}(B) = h\}| \,. \tag{3.3}$$

We know that $N(1) = 1$ (from $B = \mathbb{P}^3$), and it is not hard to determine that $N(2) = 27$ (from $\mathbb{P}^1 \times \mathbb{P}^2$, 12 distinct nontrivial $\mathbb{P}^1$ bundles over $\mathbb{P}^2$ and 14 distinct nontrivial $\mathbb{P}^2$ bundles over $\mathbb{P}^1$; there is also one toric base with $h^{1,1}(B) = 2$ and an E_8 divisor — the $\mathbb{P}^1$ bundle over $\mathbb{P}^2$ with twist 18 — that is not in the connected graph $\mathcal{C}$.) As a check on our methodology, the ratio $N(2)/N(1) = 27$ is correctly reproduced to good accuracy by Monte Carlo runs with a low bound on h.

We denote the number of bases with $h^{1,1}(B) = h$ encountered in the experiment $h^{1,1}(B) \leq m$ by $\mathcal{N}_m(h)$. The numbers are geometrically averaged among multiple runs. Then the run at $k = 1$ gives an estimate of $N(7)$, using the experimental ratio $\mathcal{N}_7(7)/\mathcal{N}_7(2)$ and the fact that $N(2) = 27$:

$$N(7) \cong 27 \cdot \frac{\mathcal{N}_7(7)}{\mathcal{N}_7(2)} \,. \tag{3.4}$$

From the run at $k = 2$ we can use the experimental value $\mathcal{N}_{12}(12)/\mathcal{N}_{12}(7)$ to estimate $N(12)$. Repeating this process we can give a rough estimate for

$$N(h) \cong 27 \times \frac{\mathcal{N}_7(7)}{\mathcal{N}_7(2)} \times \frac{\mathcal{N}_{12}(12)}{\mathcal{N}_{12}(7)} \times \cdots \times \frac{\mathcal{N}_{h'}(h')}{\mathcal{N}_{h'}(h'-5)} \times \frac{\mathcal{N}_{h'+5}(h)}{\mathcal{N}_{h'+5}(h')} \,, \tag{3.5}$$

where $h' \equiv 2 \pmod 5$ and $h - 5 < h' \leq h$. Finally when $h \geq 67$, the proportion of bases at each h is significant enough that we can employ the data from the 100 unbounded runs, and $N(h)$ can be estimated by

$$N(h) \cong N(67) \cdot \frac{\mathcal{N}_{\text{unbounded}}(h)}{\mathcal{N}_{\text{unbounded}}(67)} \,. \tag{3.6}$$

The resulting estimations of $N(h)$ are graphed in figure 10. We also plot $\log_{10}(N(h))$ in figure 11, with the standard deviation. It turns out that in the region $h \leq 35$, the number of bases grows exponentially. In the region $35 \leq h \leq 60$, the exponential growth slows down. Finally the number of bases reaches a peak at $h \cong 82$.

Summing these approximate values, we have a very rough estimate

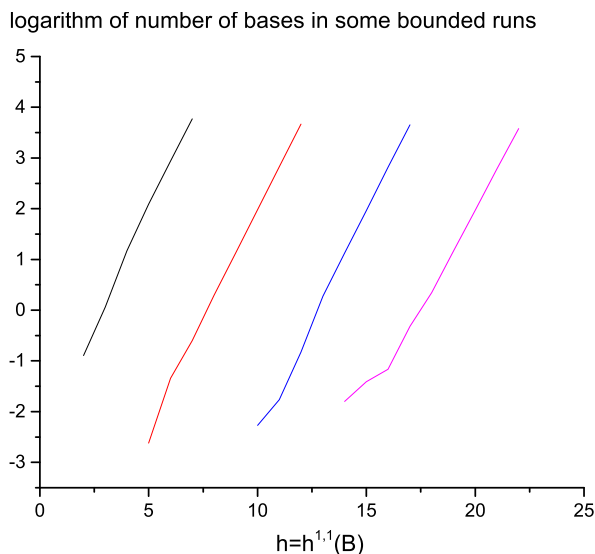$$|\mathcal{C}| = \sum_{h=1}^{\infty} \mathcal{N}(h) \sim 10^{48 \pm 2} \,. \tag{3.7}$$

Figure 9. Distributions of bases in connected sets with an upper bound $h^{1,1}(B) \leq 5k + 2$ for $k = 1, 2, 3, 4$. Only the relative numbers are plotted, so that those curves can be displaced vertically and connected.
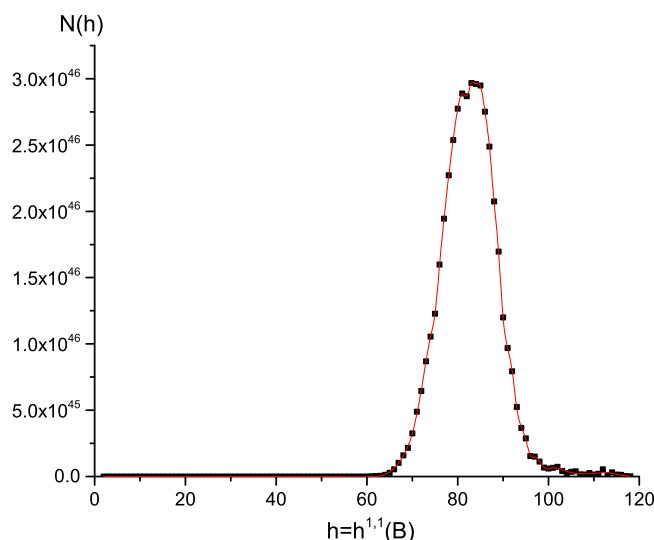

Figure 10. Rough estimation of the number of bases $B \in \mathcal{C}$ with $h^{1,1}(B) = h$.

3.2.3 Number of possible flops on each base

One possible explanation for the exponential growth of the number of bases with $h^{1,1}(B)$ is the existence of many flops (see figure 2) on typical bases with large $h^{1,1}(B)$. Since a flop does not change the rays or the set of monomials, the geometric non-Higgsable gauge group content of the associated F-theory compactification does not change under a flop. Because $v_i + v_j = v_k + v_l$, f and g also vanish to the same order on the toric curves $v_i v_j$ and $v_k v_l$. Hence if $B_1 \in \mathcal{C}$, and B_2 can be related to B_1 by a flop, then $B_2 \in \mathcal{C}$ always holds. Note, however, that because the curves lie on different combinations of divisors after a flop, the
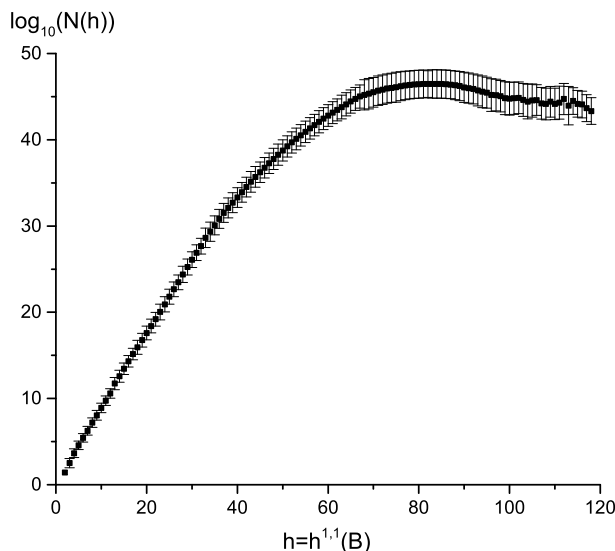
Figure 11. Rough estimation of $\log_{10}(N(h))$ with error bars, where $N(h)$ is the number of bases $B \in \mathcal{C}$ with $h^{1,1}(B) = h$.

matter content of an F-theory model, associated with the codimension two singularities on curves that live in each divisor, may change under a flop.

If there are n possible flops on a base $B \in \mathcal{C}$, and each flop is isolated, then there are 2^n bases in $\mathcal{C}$ that can be related to B by a sequence of flops. A flop can occur when 4 vertices associated with rays v_i are coplanar and connected by 2d cones as in figure 2. When more than 4 vertices are coplanar and connected, multiple connected flops can be possible. In this case, the total number of distinct bases in the set connected by flops may not be exactly 2^n. Performing a flop may, for example, destroy the possibility of others among the n possible flops. Or it may bring in new possible flops, so the 2^n is just an estimation. An example of 6 vertices, with six distinct triangulations connected by flops, is shown in figure 12. In different subsets of these configurations the number of possible flops is $n = 1, 2$, or 3, showing that 2^n can over or underestimate the actual number of configurations connected through flop sequences. All of those bases give rise to the same gauge groups and similar physics in F-theory compactifications, though precise details including the (geometric) matter spectrum may differ between the constructions. Despite the differences caused by connected sets of flops, 2^n can be viewed as a good order of magnitude estimate for the number of distinct bases associated with different triangulations of a single structure connected by flops.

The average numbers of possible flops on bases with different $h^{1,1}(B)$ are plotted in figure 13. The number of flops grows almost linearly from $h^{1,1}(B) = 50$ to $h^{1,1}(B) = 100$. Comparing to figure 11, we can see that even if we divide the total number of bases for a given $h^{1,1}(B)$ by 2^n, where n is the average number of possible flops, the number of distinct triangulation types of bases still grows exponentially. Hence there are still approximately $10^{48}/2^{20} \sim 10^{42}$ distinct bases that cannot be related by flops.
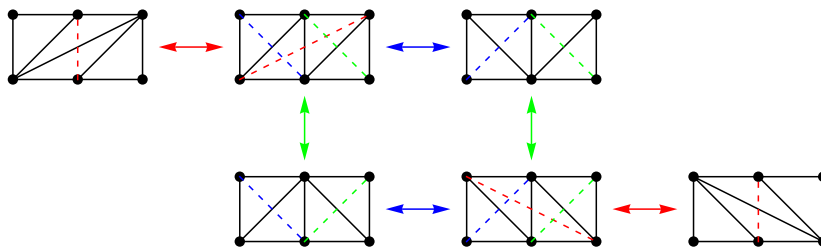
Figure 12. Different cone configurations connecting six rays associated with coplanar vertices in the lattice $N = \mathbb{Z}^3$ are connected by flops. In two of these configurations there is only one possible flop, in another two there are two possible flops, and in the other two there are three possible flops.
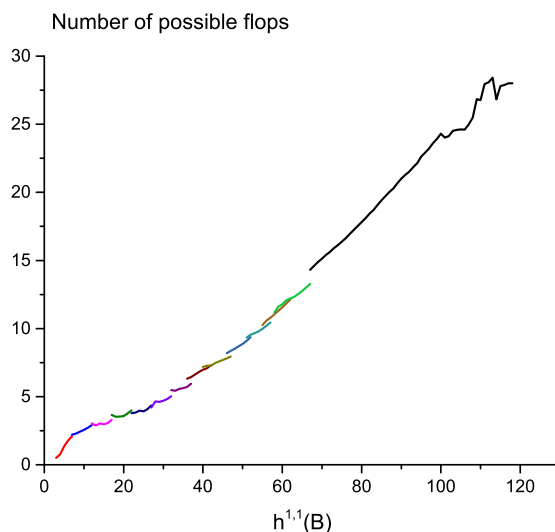

Figure 13. Average number of possible flops on B as a function of $h^{1,1}(B)$. For $h^{1,1}(B) > 67$, the numbers are computed from the 100 unbounded runs. For the lower values of $h^{1,1}(B)$, they are computed from the bounded runs.

3.3 Distribution of non-Higgsable group factors

The geometrically non-Higgsable gauge groups and matter that arise on divisors and curves in the F-theory base B provide a convenient structure with which to characterize both the geometry of elliptic Calabi-Yau manifolds and the physics of the associated F-theory compactifications [5, 7, 12–15]. While a full analysis of the physics of a given F-theory model would involve many additional considerations, including tuning of enhanced gauge symmetries or matter fields, G-flux, brane world-volume fields, etc., the non-Higgsable geometry provides a starting point for such analysis. In this section and the following section we look at generic features of non-Higgsable gauge groups that arise on the bases found in our Monte Carlo study. In section 3.5, we look at codimension two singularities associated with matter fields and other structure.
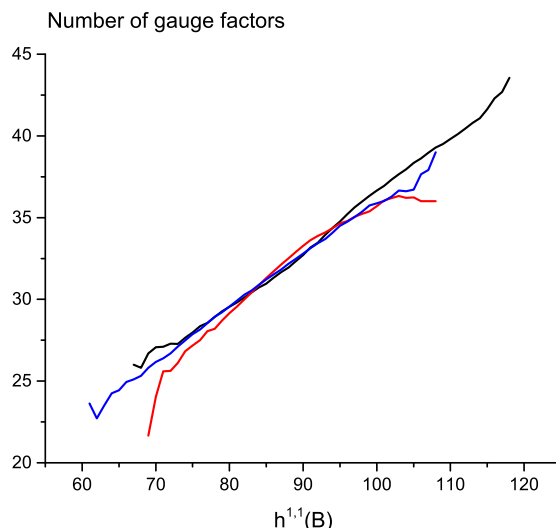
Figure 14. Average number of factors in G as a function of $h^{1,1}(B)$, in three different unbounded runs with 100,000 samples.

3.3.1 Number of factors in G

Essentially all the bases found in the Monte Carlo runs had some divisors supporting non-Higgsable gauge factors. The only exceptions were in the first few bases encountered in each run, before "thermalization".

The number of factors in G grows roughly linearly with $h^{1,1}(B)$. This is shown in figure 14 for several different individual runs, and averaged over runs in figure 15. For bases with $h^{1,1}(B)$ between 40 and 100, the fraction of divisors on any base that support a non-Higgsable gauge factor is roughly 35–40%. The fraction is slightly smaller for low $h^{1,1}(B)$, which is not surprising as the divisors can more easily have positive normal bundles when there are fewer rays in the toric fan, and non-Higgsable gauge factors are associated with negative contributions to the normal bundle [14]. Note that this fraction of divisors supporting non-Higgsable gauge factors is significantly smaller than in the case of $\mathbb{P}^1$-bundle bases studied in [15] (see figure 12 in that paper). This can be understood because of the special geometric structure of the $\mathbb{P}^1$-bundle bases, which is dominated by an essentially 2d structure of the base surface S for the $\mathbb{P}^1$ bundle, so that the statistics there are closer to what is expected from non-Higgsable groups on toric base surfaces [6], where the divisors form a linear chain, with one- or two-factor non-Higgsable clusters separated by -1 curves on surfaces of large $h^{1,1}(S)$. The smaller fraction of divisors we find in the Monte Carlo analysis is presumably a manifestation of the truly 3D nature of the toric threefold bases. An interesting question is whether this fraction will be similar for non-toric bases, which do not have the intersection structure on divisors associated with the triangulation of an S^2 by the divisor rays as in the toric threefold case.

3.3.2 Distribution of gauge factors

We have listed the average numbers of times that each individual non-Higgsable gauge group factor arises on a typical base in table 2 and figure 16. The percentage of the time
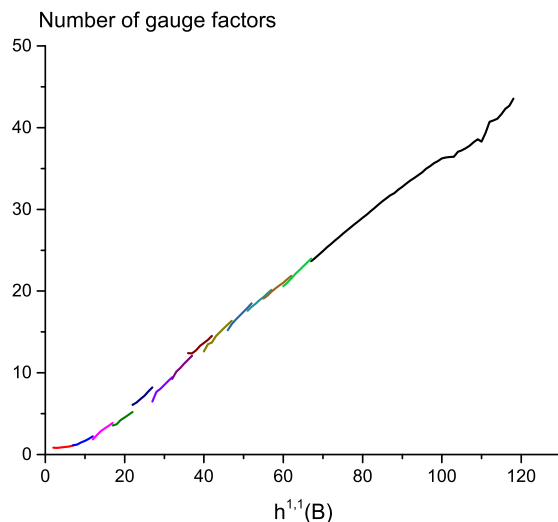
Figure 15. Average number of factors in G as a function of $h^{1,1}(B)$. For the part of the graph with $h^{1,1}(B) > 67$, averages are computed from the 100 unbounded runs. For the lower values of $h^{1,1}(B)$, averages are computed from the bounded runs.

$SU(2)_{III}$	$SU(2)_{IV}$	$SU(2)$	$SU(3)$	G_2
6.1 ± 1.7	7.5 ± 1.5	13.6 ± 1.6	2.0 ± 0.6	9.7 ± 1.8
$SO(7)$	$SO(8)$	F_4	E_6	E_7
$4 \times 10^{-6} \pm 2 \times 10^{-5}$	1.0 ± 0.6	2.8 ± 1.1	0.3 ± 0.4	0.2 ± 0.5

Table 2. Average number of times each non-Higgsable gauge group factor appears on a base, with standard deviation computed among the 100 runs.
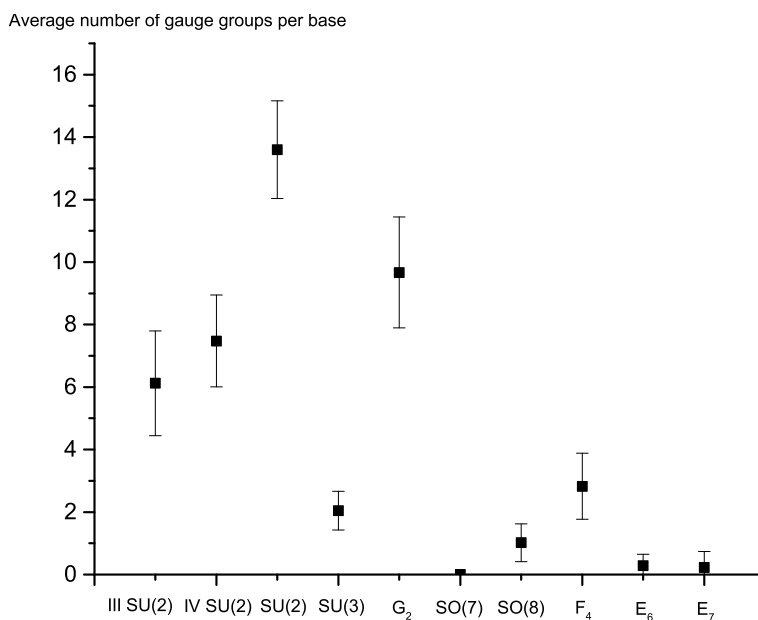

Figure 16. Average number of times each gauge group factor appears per base, with standard deviation computed among the 100 runs.

$SU(2)_{III}$	$SU(2)_{IV}$	$SU(2)$	$SU(3)$	G_2
20 ± 5	26 ± 6	46 ± 4	7 ± 3	32 ± 4
$SO(7)$	$SO(8)$	F_4	E_6	E_7
$1 \times 10^{-5} \pm 7 \times 10^{-5}$	3.4 ± 2.1	9 ± 3	0.9 ± 1.1	0.9 ± 2.3

Table 3. Average percentage of each gauge group factor, with standard deviation computed among the 100 runs.
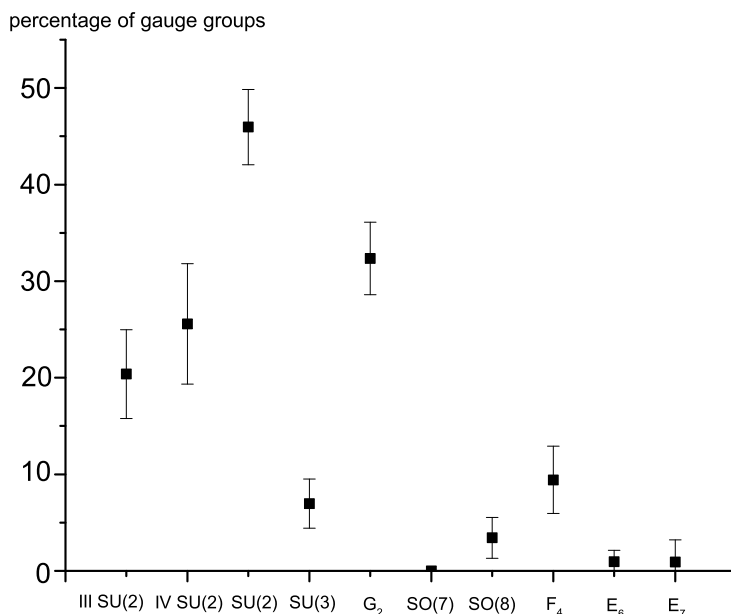

Figure 17. Average percentage appearance of each gauge group factor, with standard deviation computed among the 100 runs.

$SU(2)$	$SU(3)$	G_2	$SO(7)$	$SO(8)$	F_4	E_6	E_7
99.999 ± 0.001	83 ± 11	99.93 ± 0.07	0.0004 ± 0.002	59 ± 21	94 ± 21	26 ± 31	18 ± 37

Table 4. Average percentage of bases with a specific gauge group factor, with standard deviation computed among the 100 runs.

that each gauge factor arises among all the gauge group factors is listed in table 3 and figure 17. We also list the percentage of bases with a specific gauge group factor in table 4.

It turns out that the gauge factors $SU(2)$ and G_2 are mostly dominant. The gauge factors F_4 and $SU(3)$ also generally arise on a typical base, with an average number of appearances higher than 1 in each case. For the other gauge group factors, their appearance seems to characterize some "local feature" of the part of landscape covered by a particular run. The gauge group $SO(7)$ is the most rare one; from these statistics, on a typical base one does not expect the appearance of $SO(7)$.

Comparing to the distribution of gauge factors found on $\mathbb{P}^1$-bundle bases [15], the percentage of $SU(3)$, $SO(8)$ and E_6 gauge groups are much higher than the corresponding total percentage values in table 3 of [15]. But the percentage of $SO(7)$ and E_7 gauge factors

SU(2) × SU(2)	SU(3) × SU(2)	SU(3) × SU(3)	G_2 × SU(2)	SO(7) × SU(2)
7.6 ± 1.9	2.4 ± 0.9	0.4 ± 0.4	14 ± 3	0 ± 0

Table 5. Average number of appearances of each gauge pair on a base, with standard deviation computed among the 100 runs.

found here are much lower. Because we do not move across regions with codimension-2 (4,6) singularities, it is natural to expect that gauge groups with high rank such as E_7 and E_8 will be much rarer in our Monte Carlo analysis. The relative frequency of SO(7) factors in $\mathbb{P}^1$-bundle bases likely comes from the basically 2d nature of the bases in that case. SU(2) × SO(7) × SU(2) is a standard non-Higgsable cluster that arises on 2d base surfaces for elliptic Calabi-Yau threefolds that contain a chain of curves of self-intersections $-2, -3, -2$ [5], and if such a sequence of curves appears in the base S supporting the $\mathbb{P}^1$ bundle the same gauge group combination can appear as a non-Higgsable structure in the resulting threefold base when the twist of the $\mathbb{P}^1$ bundle over that non-Higgsable cluster is minimal. The absence of these factors in our Monte Carlo study reflects the more intrinsically 3d structure of the bases explored here. This explanation agrees with the observation made in [15], that the percentages of non-Higgsable gauge group factors that arise on the sections of the $\mathbb{P}^1$ bundle bases (last line of table 3 in that paper) are much higher for SU(3), SO(8) and E_6 factors than on other divisors, which makes sense since the sections are described geometrically by a broader class of surfaces that locally corresponds more closely to the general set of toric divisors in the toric threefold bases explored in the Monte Carlo analysis here. The percentages of gauge groups we find here indeed correspond reasonably well with those found in [15] when restricted to sections of the $\mathbb{P}^1$-bundle base, suggesting that the broad features of these results are fairly generic. In particular, the dominance of G_2 and SU(2), the moderate level of appearance of SU(3), SO(8) and E_6, and the relative rarity of SO(7) are common features to these distributions.

3.3.3 Distribution of gauge pairs

As discussed in [14], the only possible configurations of two non-Higgsable gauge factors located on neighboring divisors are:

$$\mathrm{SU}(2) \times \mathrm{SU}(2)\,,\ \mathrm{SU}(3) \times \mathrm{SU}(2)\,,\ \mathrm{SU}(3) \times \mathrm{SU}(3)\,,\ G_2 \times \mathrm{SU}(2)\,,\ \mathrm{SO}(7) \times \mathrm{SU}(2) \quad (3.8)$$

This follows from the requirement that there is not a (4,6) singularity on the intersection of the two divisors, along with monodromy conditions. Such gauge pairs are naturally associated with codimension two singularities supporting (geometric) matter that transforms as a field charged under both factors.

We have listed the average number of times each gauge pair arises on a typical base in table 5 and figure 18. The percentage of each gauge pair among all the gauge pairs is listed in table 6 and figure 19. We also list the percentage of bases with a specific gauge pair in table 7.

The data on gauge pairs elaborates on the results presented in the last section. The most dominant gauge pairs are SU(2) × SU(2) and G_2 × SU(2); SU(3) × SU(2) appears
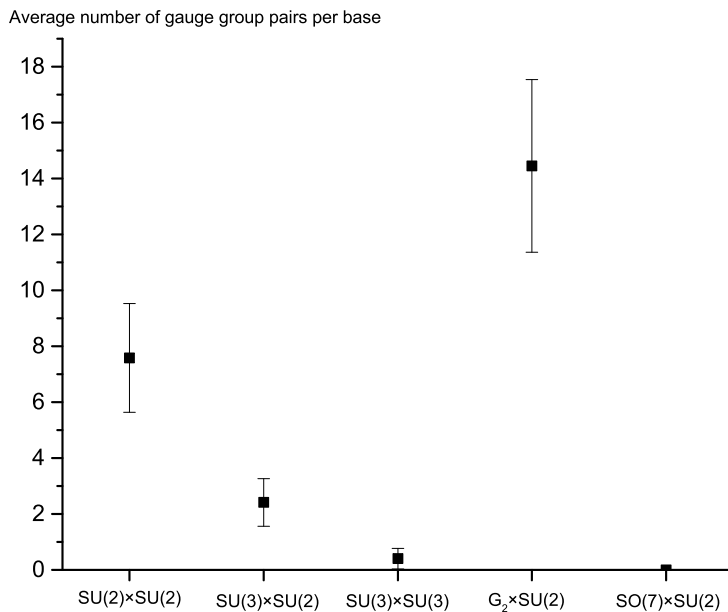
Figure 18. Average number of appearances of each gauge pair per base, with standard deviation computed among the 100 runs.

$SU(2) \times SU(2)$	$SU(3) \times SU(2)$	$SU(3) \times SU(3)$	$G_2 \times SU(2)$	$SO(7) \times SU(2)$
31 ± 5	10 ± 3	1.7 ± 2.4	58 ± 6	0 ± 0

Table 6. Average percentage of each gauge pair, with standard deviation computed among the 100 runs.
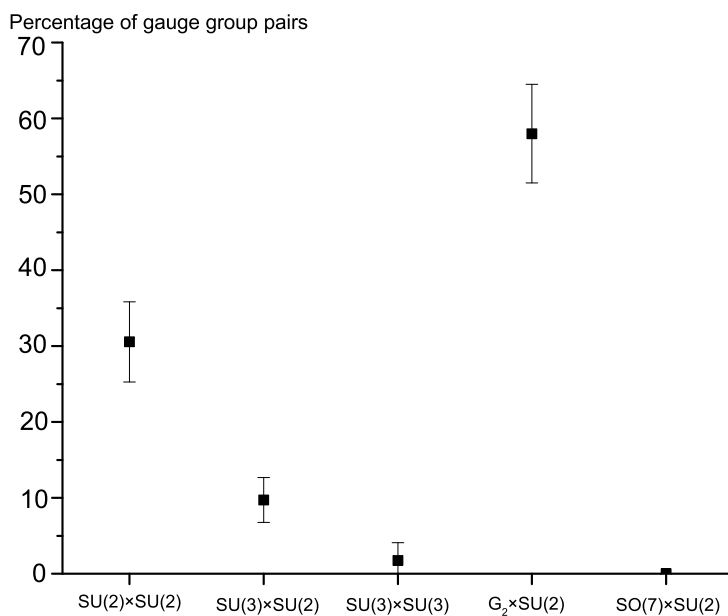

Figure 19. Average percentage of each gauge pair, with standard deviation computed among the 100 runs.

$SU(2) \times SU(2)$	$SU(3) \times SU(2)$	$SU(3) \times SU(3)$	$G_2 \times SU(2)$	$SO(7) \times SU(2)$
98 ± 6	76 ± 14	28 ± 16	99.9 ± 0.7	0 ± 0

Table 7. Average percentage of bases with a specific gauge pair, with standard deviation computed among the 100 runs.

moderately frequently, and the gauge pair $SO(7) \times SU(2)$ is so rare that it never appears in our sampling runs. This indicates that the average number of $SO(7) \times SU(2)$ pairs on a typical base could be lower than 1×10^{-7}. The qualitative features of the distribution on pairs match with what was found in [15] for gauge pairs on divisors of which one is a section of a $\mathbb{P}^1$-bundle base.

An interesting feature in the statistics is that for a typical base, the gauge pair $SU(3) \times SU(2)$ appears more than once, and more than half of bases ($\sim 76\%$) support at least one $SU(3) \times SU(2)$ gauge pair. Such a non-Higgsable gauge product could act as the non-Abelian part of the standard model gauge group in a MSSM-like scenario [13]. We leave the detailed construction of such phenomenological models to future work.

3.4 Clusters

As discussed in [14], there are many possible non-Higgsable clusters with size greater than two in 4d F-theory. Since the possible configurations may be essentially arbitrarily complicated, bounded only by the hypothetically finite number of threefold bases that support elliptic Calabi-Yau fourfolds, it is not feasible to classify all the large clusters. We only present some statistical data here. On average, each base has a non-Higgsable gauge group with roughly 30 simple non-Abelian factors, of which 6.6 ± 1.6 are single gauge factors that are not contained in any larger non-Higgsable clusters. Those gauge group components automatically include all the $SO(8)$, F_4, E_6 and E_7 gauge factors. On each base there are 0.9 ± 0.5 non-Higgsable clusters with size equal to two, and 2.0 ± 0.5 larger clusters. We plot the average numbers of non-Higgsable clusters of different size, on a base in figure 20. The average cluster size is 3.3 ± 0.8, including the single gauge groups. On each base we can find the largest non-Higgsable cluster, and its average size is 16 ± 4. All the standard deviations are computed among the 100 runs.

This means that a typical base in 4d F-theory contains very large non-Higgsable clusters, which contain most of the gauge factors $SU(2)$, $SU(3)$ and G_2. A sample of the set of non-Higgsable clusters for a typical base encountered in one of the Monte Carlo runs is shown in figure 21. This example illustrates the complexity of the large clusters. This base supports a non-Higgsable gauge group with 30 non-Abelian simple factors, with one cluster of size 16, one cluster of size 5, one cluster of size 2, and 7 isolated gauge factors. The clusters of size 16 and 5 illustrate the branching and looping possibilities of NHC's for 4d F-theory models discussed in [14]. The gauge factor $SU(3)$ appears 3 times. The non-Higgsable gauge pair $SU(3) \times SU(2)$ appears 6 times, once as an isolated pair and five times in the cluster of size 16. If the non-Abelian part of the standard model were realized on the isolated pair, all other gauge factors not broken by fluxes would play a role in hidden dark matter sectors; if the standard model $SU(3) \times SU(2)$ came from one of the pairs in
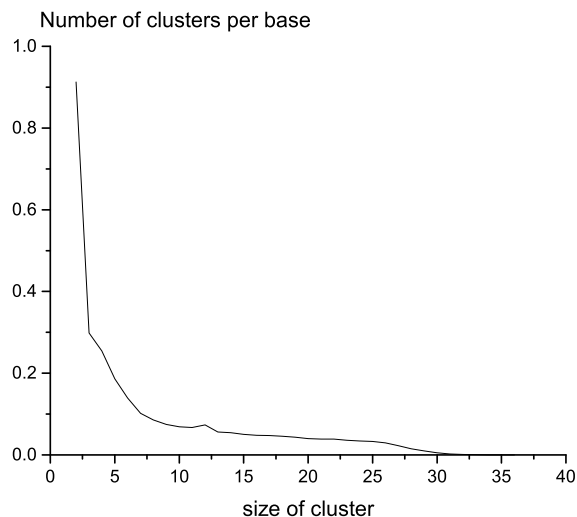
Figure 20. The average number of non-Higgsable clusters of each size on a base.
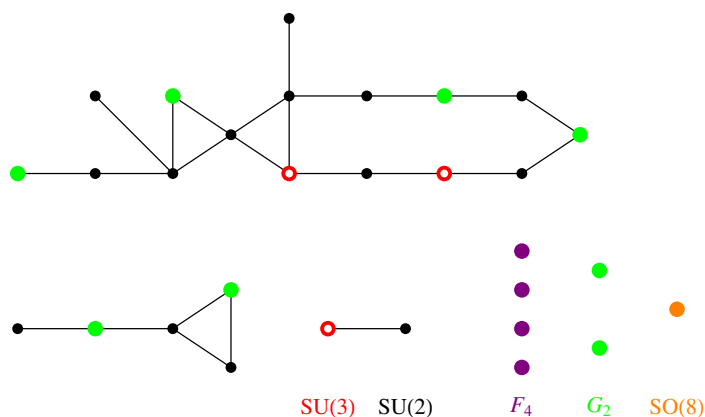

Figure 21. The non-Higgsable clusters of a fairly typical base actually encountered in the Monte Carlo study of toric threefold bases. This base has $h^{1,1}(B) = 82$ and supports a 30-factor gauge group $SU(2)^{14} \times G_2^8 \times SU(3)^3 \times F_4^4 \times SO(8)$, which contains six $SU(3) \times SU(2)$ factors with jointly charged matter.

the size 16 cluster, there could be WIMP dark matter charged under the $SU(2)$ and dark sector $SU(2)$, $SU(3)$ or G_2 groups.

Among all the 10^7 bases encountered in the 100 Monte Carlo runs, the largest non-Higgsable cluster was one of size 37, with gauge group $SU(2)^{19} \times G_2^{14} \times SU(3)^4$ (see figure 22).

3.5 Codimension two singularities and matter curves

3.5.1 Matter charged under gauge group(s)

In F-theory the codimension-two locus of singular fibers on the base B generally corresponds to matter in the 4d supergravity theory. In type IIB language such singularities arise at the intersection of two sets of 7-branes. If one set of 7-branes carries a non-Abelian gauge group G, then the open strings attached between the two sets of 7-branes give rise
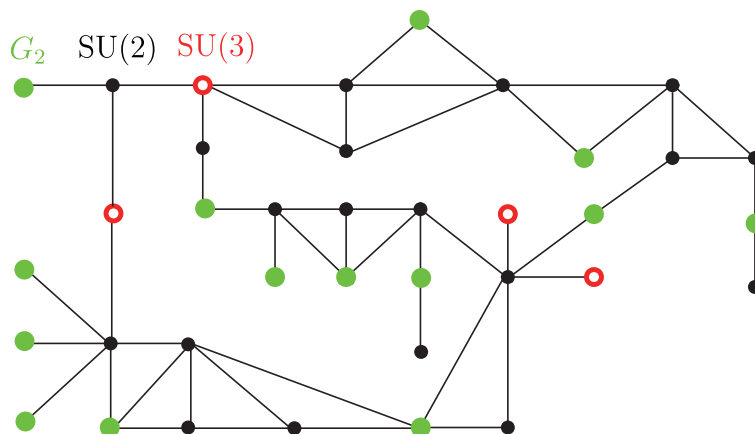
Figure 22. The largest non-Higgsable cluster we have encountered in our search. It contains a 37-factor gauge group $SU(2)^{19} \times G_2^{14} \times SU(3)^4$.

$SU(2)_{III}$	$SU(2)_{IV}$	$SU(2)$	$SU(3)$	G_2
93	99.98	97	93	99.6
$SO(7)$	$SO(8)$	F_4	E_6	E_7
100	70	99.985	94	84

Table 8. Percentage of gauge groups with matter charged under this single gauge factor.

to matter fields living in some representation R of G. In 4d F-theory the chiral index of the charged matter in some specific representation can be related to the G-flux in the M-theory description of the theory [47–51]. We do not give any quantative description of matter curves in specific representations here. On our 3d toric bases B there are two different types of matter curves. The first case is the toric curve $D_i D_j$ where D_i and D_j possess non-Abelian gauge groups G_1 and G_2 respectively. Then generally there will be quiver matter in the representation (R_1, R_2) of G_1 and G_2. For toric constructions the matter is generally in the bifundamental representation. The second case is when the vanishing locus of Δ on a divisor D_i contains a curve C, where D_i possesses a non-Abelian gauge group G, but no other divisor carrying a non-Abelian factor passes through C. Then there will be matter charged under the single gauge group G. This kind of matter appears typically when the leading coefficient Δ_p in the expansion

$$\Delta = \Delta_p w^p + \Delta_{p+1} w^{p+1} + \dots \tag{3.9}$$

around the divisor $D = \{w = 0\}$ contains more than one monomial. For a given divisor D_i, those two different types of matter curves may simultaneously exist.

We list the proportion of gauge groups with those two types of matter in tables 8–10. One can see that almost all the divisors with non-Higgsable gauge groups can have charged matter on them.

We have also counted the average number of each type of possible dark sector gauge groups adjacent to each of the SU(2) factors in a gauge pair SU(3) × SU(2). Such gauge factors are generally associated with charged matter that is also charged under

$SU(2)_{III}$	$SU(2)_{IV}$	$SU(2)$	$SU(3)$	G_2	$SO(7)$
98.7	95	97	86	84	0

Table 9. Percentage of gauge groups with quiver matter charged under this gauge factor, or equivalently, gauge groups inside some non-Higgsable cluster.

$SU(2)_{III}$	$SU(2)_{IV}$	$SU(2)$	$SU(3)$	G_2
99.987	99.999	99.994	99.90	99.95
$SO(7)$	$SO(8)$	F_4	E_6	E_7
100	70	99.99	94	84

Table 10. Percentage of gauge groups with any type of matter.

$SU(2)$	$SU(3)$	G_2
0.86 ± 0.23	0.07 ± 0.04	0.74 ± 0.19

Table 11. Average number of each type of "dark sector" gauge factor connected to each $SU(2)$ in gauge pairs $SU(3) \times SU(2)$, with standard deviation computed among the 100 runs.

the $SU(2)$ factor. These are listed in table 11. Similar to the distribution of gauge pairs, the gauge groups $SU(2)$ and G_2 are dominant here.

3.5.2 Codimension two singularities without gauge groups

Besides those possibilities, there are also enhanced codimension-two singularities without any gauge group. For example we consider the following base B_1, a $\mathbb{P}^1$ bundle over $\mathbb{F}_1$, with 6 toric divisors:

$$
\begin{aligned}
v_1 &= (0,0,1), & v_2 &= (0,0,-1), & v_3 &= (0,1,0), \\
v_4 &= (1,0,0), & v_5 &= (0,-1,0), & v_6 &= (-1,-1,2).
\end{aligned}
\tag{3.10}
$$

The set of 3d cones is:

$$
\{v_1 v_3 v_4, v_2 v_3 v_4, v_2 v_4 v_5, v_2 v_5 v_6, v_1 v_3 v_6, v_1 v_4 v_5, v_1 v_5 v_6, v_2 v_3 v_6\}.
\tag{3.11}
$$

The orders of vanishing for f, g and Δ on each of these divisors are identically zero, so there are no non-Higgsable gauge group factors supported on any toric divisors in the generic elliptic fibration over the base B_1. However, on the toric curve $v_1 v_5$, f, g and Δ vanish to order $(2, 3, 6)$. We can explicitly write down the Weierstrass form near this curve $s = t = 0$:

$$
y^2 = x^3 + (a_0 s^2 + a_1 st^2 + a_2 t^4)x + (b_1 s^3 + b_2 s^2 t^2 + b_3 st^4 + b_4 t^6)
\tag{3.12}
$$

The discriminant

$$
\Delta = c_1 s^6 + c_2 t^{12} + \dots
\tag{3.13}
$$

has a cusp at the point $s = t = 0$. In type IIB language this configuration corresponds to many I_1 7-branes intersecting on a toric curve on B_1, and there is singularity enhancement on that curve. This is a novel type of singularity, which may not be described by the

standard Kodaira ADE classification. Systematic approaches to resolving codimension two singularities have been described in [52–60]. For the Weierstrass form (3.12), however, it seems that the singularity at $x = y = s = t = 0$ cannot be resolved using these methods. Another available technique that may be useful in understanding these singularities is the string junction method, which involves the (non-Kähler) deformation of the Weierstrass model [62]. It seems, however, that these represent singularities that cannot be resolved to a total space that is a Calabi-Yau fourfold. The physical relevance of those codimension-two singularities is also not clear. Naively they correspond to some localized neutral matter. Codimension two and higher singularities without an apparent Calabi-Yau resolution have arisen in several other contexts in F-theory. Codimension 3 singularities where f, g vanish to orders of at least (4, 6) but less than (8, 12) do not have a simple Calabi-Yau resolution but may be benign [35]. Codimension two singularities without a CY resolution have appeared associated with matter charged under discrete gauge groups [63–68]. Codimension two singularities without a CY resolution are also encountered in generalizations of the Schoen construction [69]. It seems likely that many of these singularities are benign from the F-theory point of view, although they may require a more sophisticated method of analysis from the usual perspective of M-theory on a smooth Calabi-Yau; for example they may represent cycles that are driven to vanish by their curvature, in any supersymmetric vacuum. Singularities of this type that cannot be resolved to a Calabi-Yau total space were considered in [61]. These codimension two singularities that we encounter on toric bases, which do not admit a flat Calabi-Yau resolution, may simply be a necessary feature of general 4d F-theory models. This kind of possibility was also discussed previously in [16] in a related context, where it was pointed out that even when there is no geometric Calabi-Yau resolution of a singular model, sensible physical features of the model can be computed for e.g. Landau-Ginzburg models. Thus, we proceed under the assumption that these codimension two singularities are acceptable features of 4d F-theory models, though their physical interpretation remains to be fully elucidated.

In the current Monte Carlo approach we have analyzed the frequency of occurrence of those toric cusp curves. We count the number of toric curves $v_i v_j$ where $\mathrm{ord}_{D_i}(f) = \mathrm{ord}_{D_i}(g) = \mathrm{ord}_{D_j}(f) = \mathrm{ord}_{D_j}(g) = 0$, $\mathrm{ord}_{D_i D_j}(f) \geq 1$ and $\mathrm{ord}_{D_i D_j}(g) \geq 2$. Averaging over the 100 unbounded runs, there are 2.7 ± 1.6 toric curves of this type on each base, which implies that this phenomenon is quite general. Thus, a typical base in the set we have considered has some unusual codimension two singularities that do not appear to admit a smooth resolution to give a total space that is Calabi-Yau, but which seem likely to be acceptable features of 4D F-theory geometries.

4 Conclusions

We have used a Monte Carlo approach to explore a large class of threefold bases for F-theory compactifications to four dimensions. The bases we have considered are smooth toric threefolds that are connected through a series of blow-up and blow-down transitions to $\mathbb{P}^3$ without passing through intermediate bases with $(4, 6)$ curves. We estimate that this set $\mathcal{C}$ contains on the order of 10^{48} distinct threefold bases. This is much larger

than the known and fully enumerated set of roughly 10^4 analogous connected toric base surfaces that support elliptic Calabi-Yau threefolds. The generic elliptically fibered Calabi-Yau fourfolds over the threefold bases in $\mathcal{C}$ give roughly 10^{48} elliptically fibered Calabi-Yau fourfolds. While some fourfolds may admit multiple distinct elliptic fibrations, this number still should act as a reasonable lower bound for the number of possible distinct elliptic Calabi-Yau fourfolds. Modifying the approach used here slightly, it is straightforward to systematically construct all the toric threefold bases in the connected set up to any given value of $h^{1,1}(B)$. Such an analysis could be implemented and would be bounded only by computational resources; for example, computing the first 10^9 bases would reach to roughly $h^{1,1}(B) \cong 10$. We have considered the gauge groups and matter that are supported by geometric non-Higgsable clusters over the bases explored. A typical base has a non-Higgsable gauge group with roughly 30 factors, dominated by SU(2) and G_2, with some SU(3) and other factors arising. Roughly 10% of connected group factor pairs are SU(3) × SU(2) pairs.

The set that we have explored here represents an enormous family of elliptic Calabi-Yau fourfolds. For elliptic Calabi-Yau threefolds, it is known that the number of distinct topological types is finite [70], and that all are connected through extremal transitions, through the minimal model theory for the base surfaces [29]. This makes possible in principle a complete and systematic classification of all elliptic Calabi-Yau threefolds, for which the numbers involved do not seem prohibitive and towards which substantial progress has been made [6–10]. For fourfolds, however, beyond the apparently prohibitive size of the number of distinct topologies involved, there are a number of further theoretical steps needed to get a systematic handle on the set of possibilities. We mention here briefly some things that were not done in this work that would represent further progress in this direction. First, there is no proof of finiteness for elliptic Calabi-Yau fourfolds, and the analogue of the minimal surfaces for threefold bases has not been worked out systematically. While the observation that the set we have explored here connects together all the known toric threefold bases with small $h^{1,1}(B)$ except those with E_8 factors that cannot be reached except through intermediate threefolds with $(4, 6)$ curves, suggesting that all toric threefold bases may be connected through extremal transitions, this has not been proven even with the restriction to toric structure. It would be nice at least to generalize the analysis done here to include almost-toric bases that have E_8 factors and $(4, 6)$ curves, as has been done in the case of base surfaces, since such bases seem to play an important role for threefolds and fourfolds at large Hodge numbers. Over each given threefold base, in general a variety of elliptic Calabi-Yau fourfolds can be constructed by tuning different codimension one and two singularities, corresponding to Higgsable gauge groups and matter in the F-theory picture. For many threefold bases this can give rise to a vast array of distinct elliptic Calabi-Yau fourfolds. A systematic analysis of such tuning would help to indicate how much larger the complete set of elliptic fourfolds might be than the set of base threefolds considered here. A systematic approach to tuning in the case of elliptic CY threefolds was described, for example, in [9]. Another question is the extent to which toric threefolds are a representative sample of the complete set of threefold bases that support elliptic Calabi-Yau fourfolds. For elliptic CY threefolds, a systematic analysis of non-toric bases [10] shows

that, at least at large $h^{2,1}$, toric base surfaces form a good representative sample of the full set of non-toric bases, but a similar analysis for threefold bases would be substantially more complex as it would involve blowing up curves in addition to points.

Finally, a few words regarding the physical relevance of the distribution we have sampled here. The Monte Carlo we have carried out samples each distinct threefold base B with a weight proportional to its number of allowed neighbors, which we have used to compute statistical averages based on an equal weighting of each toric threefold base. There is no physical reason why this is a correct weighting, this is simply a mathematical formulation of a simple weighting factor that allows us to study typical features of the ensemble based on an equal weighting of base threefolds. A proper weighting of bases for physics is not fully understood and would depend on the detailed global dynamics of string theory. The effects of G-flux and world-volume brane dynamics would also need to be included to systematically analyze the set of possibilities from a physics perspective. The most plausible approach advanced so far for understanding physical vacuum distributions in F-theory is the statistical approach to flux vacua developed by Ashok, Douglas and Denef [71, 72] (see [73–75] for a recent application in the F-theory context, and [11, 76] for pedagogical reviews). We leave a consideration of the effects of fluxes on the distribution of vacua in the context developed here for future work.

Acknowledgments

References

[1] C. Vafa, *Evidence for F-theory*, *Nucl. Phys.* **B 469** (1996) 403 [hep-th/9602022] [INSPIRE].

[2] D.R. Morrison and C. Vafa, *Compactifications of F-theory on Calabi-Yau threefolds. 1*, *Nucl. Phys.* **B 473** (1996) 74 [hep-th/9602114] [INSPIRE].

[3] D.R. Morrison and C. Vafa, *Compactifications of F-theory on Calabi-Yau threefolds. 2.*, *Nucl. Phys.* **B 476** (1996) 437 [hep-th/9603161] [INSPIRE].

[4] V. Kumar, D.R. Morrison and W. Taylor, *Global aspects of the space of* 6D $N = 1$ *supergravities*, *JHEP* **11** (2010) 118 [arXiv:1008.1062] [INSPIRE].

[5] D.R. Morrison and W. Taylor, *Classifying bases for* 6D *F-theory models*, *Central Eur. J. Phys.* **10** (2012) 1072 [arXiv:1201.1943] [INSPIRE].

[6] D.R. Morrison and W. Taylor, *Toric bases for* 6D *F-theory models*, *Fortsch. Phys.* **60** (2012) 1187 [arXiv:1204.0283] [INSPIRE].

[7] W. Taylor, *On the Hodge structure of elliptically fibered Calabi-Yau threefolds*, *JHEP* **08** (2012) 032 [arXiv:1205.0952] [INSPIRE].

[8] G. Martini and W. Taylor, *6D F-theory models and elliptically fibered Calabi-Yau threefolds over semi-toric base surfaces*, *JHEP* **06** (2015) 061 [arXiv:1404.6300] [INSPIRE].

[9] S.B. Johnson and W. Taylor, *Calabi-Yau threefolds with large $h^{2,1}$*, *JHEP* **10** (2014) 23 [arXiv:1406.0514] [INSPIRE].

[10] W. Taylor and Y.-N. Wang, *Non-toric Bases for Elliptic Calabi-Yau Threefolds and 6D F-theory Vacua*, arXiv:1504.07689 [INSPIRE].

[11] F. Denef, *Les Houches Lectures on Constructing String Vacua*, arXiv:0803.1194 [INSPIRE].

[12] L.B. Anderson and W. Taylor, *Geometric constraints in dual F-theory and heterotic string compactifications*, *JHEP* **08** (2014) 025 [arXiv:1405.2074] [INSPIRE].

[13] A. Grassi, J. Halverson, J. Shaneson and W. Taylor, *Non-Higgsable QCD and the Standard Model Spectrum in F-theory*, *JHEP* **01** (2015) 086 [arXiv:1409.8295] [INSPIRE].

[14] D.R. Morrison and W. Taylor, *Non-Higgsable clusters for 4D F-theory models*, *JHEP* **05** (2015) 080 [arXiv:1412.6112] [INSPIRE].

[15] J. Halverson and W. Taylor, *$\mathbb{P}^1$-bundle bases and the prevalence of non-Higgsable structure in 4D F-theory models*, *JHEP* **09** (2015) 086 [arXiv:1506.03204] [INSPIRE].

[16] A. Klemm, B. Lian, S.S. Roan and S.-T. Yau, *Calabi-Yau fourfolds for M-theory and F-theory compactifications*, *Nucl. Phys.* **B 518** (1998) 515 [hep-th/9701023] [INSPIRE].

[17] K. Mohri, *F theory vacua in four-dimensions and toric threefolds*, *Int. J. Mod. Phys.* **A 14** (1999) 845 [hep-th/9701147] [INSPIRE].

[18] P. Berglund and P. Mayr, *Heterotic string / F theory duality from mirror symmetry*, *Adv. Theor. Math. Phys.* **2** (1999) 1307 [hep-th/9811217] [INSPIRE].

[19] T.W. Grimm and W. Taylor, *Structure in 6D and 4D $N = 1$ supergravity theories from F-theory*, *JHEP* **10** (2012) 105 [arXiv:1204.3092] [INSPIRE].

[20] D.R. Morrison, *TASI lectures on compactification and duality*, hep-th/0411120 [INSPIRE].

[21] W. Taylor, *TASI Lectures on Supergravity and String Vacua in Various Dimensions*, arXiv:1104.2051 [INSPIRE].

[22] K. Kodaira, *On compact analytic surfaces. II, III*, *Ann. of Math.* **77** (1963) 563, **78** (1963) 1.

[23] J. Tate, *Algorithm for determining the type of a singular fiber in an elliptic pencil, Modular functions of one variable, IV*, Proceedings of *Internat. Summer School*, Univ. Antwerp, Antwerp, Belgium, 1972, *Lecture Notes in Math.* **476** (1975) 33.

[24] M. Bershadsky, K.A. Intriligator, S. Kachru, D.R. Morrison, V. Sadov and C. Vafa, *Geometric singularities and enhanced gauge symmetries*, *Nucl. Phys.* **B 481** (1996) 215 [hep-th/9605200] [INSPIRE].

[25] S. Katz, D.R. Morrison, S. Schäfer-Nameki and J. Sully, *Tate's algorithm and F-theory*, *JHEP* **08** (2011) 094 [arXiv:1106.3854] [INSPIRE].

[26] A. Grassi and D.R. Morrison, *Anomalies and the Euler characteristic of elliptic Calabi-Yau threefolds*, *Commun. Num. Theor. Phys.* **6** (2012) 51 [arXiv:1109.0042] [INSPIRE].

[27] W. Fulton. *Introduction to toric varieties. No. 131*, Princeton University Press, (1993).

[28] W.P. Barth, K. Hulek, C.A.M. Peters, A. Van de Ven, *Compact complex surfaces*, Springer, (2004).

[29] A. Grassi, *On minimal models of elliptic threefolds*, *Math. Ann.* **290** (1991) 287.

[30] N. Seiberg and E. Witten, *Comments on string dynamics in six-dimensions*, *Nucl. Phys.* **B 471** (1996) 121 [`hep-th/9603003`] [InSPIRE].

[31] N. Seiberg, *Nontrivial fixed points of the renormalization group in six-dimensions*, *Phys. Lett.* **B 390** (1997) 169 [`hep-th/9609161`] [InSPIRE].

[32] J.J. Heckman, D.R. Morrison and C. Vafa, *On the Classification of 6D SCFTs and Generalized ADE Orbifolds*, *JHEP* **05** (2014) 028 [*Erratum ibid.* **1506** (2015) 017] [`arXiv:1312.5746`] [InSPIRE].

[33] M. Del Zotto, J.J. Heckman, D.R. Morrison and D.S. Park, *6D SCFTs and Gravity*, *JHEP* **06** (2015) 158 [`arXiv:1412.6526`] [InSPIRE].

[34] K. Matsuki, *Introduction to the Mori Program*, Springer-Verlag, Berlin Germany (2002).

[35] P. Candelas, D.-E. Diaconescu, B. Florea, D.R. Morrison and G. Rajesh, *Codimension three bundle singularities in F-theory*, *JHEP* **06** (2002) 014 [`hep-th/0009228`] [InSPIRE].

[36] R. Wazir, *Arithmetic on elliptic threefolds*, *Compos. Math.* **140** (2004) 567.

[37] A. Braun, W. Taylor and Y. Wang, to appear.

[38] M. Lynker, R. Schimmrigk and A. Wisskirchen, *Landau-Ginzburg vacua of string, M-theory and F-theory at c = 12*, *Nucl. Phys.* **B 550** (1999) 123 [`hep-th/9812195`] [InSPIRE].

[39] M. Kreuzer and H. Skarke, *Calabi-Yau four folds and toric fibrations*, *J. Geom. Phys.* **26** (1998) 272 [`hep-th/9701175`] [InSPIRE].

[40] http://hep.itp.tuwien.ac.at/~kreuzer/CY/.

[41] H. Skarke, *Weight systems for toric Calabi-Yau varieties and reflexivity of Newton polyhedra*, *Mod. Phys. Lett.* **A 11** (1996) 1637 [`alg-geom/9603007`] [InSPIRE].

[42] A.C. Avram, M. Kreuzer, M. Mandelberg and H. Skarke, *Searching for K3 fibrations*, *Nucl. Phys.* **B 494** (1997) 567 [`hep-th/9610154`] [InSPIRE].

[43] M. Kreuzer and H. Skarke, *Complete classification of reflexive polyhedra in four-dimensions*, *Adv. Theor. Math. Phys.* **4** (2002) 1209 [`hep-th/0002240`] [InSPIRE].

[44] P. Candelas, A. Constantin and H. Skarke, *An Abundance of K3 Fibrations from Polyhedra with Interchangeable Parts*, *Commun. Math. Phys.* **324** (2013) 937 [`arXiv:1207.4792`] [InSPIRE].

[45] J. Gray, A.S. Haupt and A. Lukas, *Topological Invariants and Fibration Structure of Complete Intersection Calabi-Yau Four-Folds*, *JHEP* **09** (2014) 093 [`arXiv:1405.2073`] [InSPIRE].

[46] L.B. Anderson, F. Apruzzi, X. Gao, J. Gray and S.-J. Lee, *A New Construction of Calabi-Yau Manifolds: Generalized CICYs*, `arXiv:1507.03235` [InSPIRE].

[47] R. Donagi and M. Wijnholt, *Model Building with F-theory*, *Adv. Theor. Math. Phys.* **15** (2011) 1237 [`arXiv:0802.2969`] [InSPIRE].

[48] C. Beasley, J.J. Heckman and C. Vafa, *GUTs and Exceptional Branes in F-theory – I*, *JHEP* **01** (2009) 058 [`arXiv:0802.3391`] [InSPIRE].

[49] C. Beasley, J.J. Heckman and C. Vafa, *GUTs and Exceptional Branes in F-theory – II: Experimental Predictions*, *JHEP* **01** (2009) 059 [arXiv:0806.0102] [INSPIRE].

[50] T.W. Grimm, *The $N = 1$ effective action of F-theory compactifications*, *Nucl. Phys.* **B 845** (2011) 48 [arXiv:1008.4133] [INSPIRE].

[51] T.W. Grimm and H. Hayashi, *F-theory fluxes, Chirality and Chern-Simons theories*, *JHEP* **03** (2012) 027 [arXiv:1111.1232] [INSPIRE].

[52] S.H. Katz and C. Vafa, *Matter from geometry*, *Nucl. Phys.* **B 497** (1997) 146 [hep-th/9606086] [INSPIRE].

[53] D.R. Morrison and W. Taylor, *Matter and singularities*, *JHEP* **01** (2012) 022 [arXiv:1106.3563] [INSPIRE].

[54] M. Esole and S.-T. Yau, *Small resolutions of* SU(5)*-models in F-theory*, *Adv. Theor. Math. Phys.* **17** (2013) 1195 [arXiv:1107.0733] [INSPIRE].

[55] C. Lawrie and S. Schäfer-Nameki, *The Tate Form on Steroids: Resolution and Higher Codimension Fibers*, *JHEP* **04** (2013) 061 [arXiv:1212.2949] [INSPIRE].

[56] H. Hayashi, C. Lawrie and S. Schäfer-Nameki, *Phases, Flops and F-theory:* SU(5) *Gauge Theories*, *JHEP* **10** (2013) 046 [arXiv:1304.1678] [INSPIRE].

[57] H. Hayashi, C. Lawrie, D.R. Morrison and S. Schäfer-Nameki, *Box Graphs and Singular Fibers*, *JHEP* **05** (2014) 048 [arXiv:1402.2653] [INSPIRE].

[58] M. Esole, S.-H. Shao and S.-T. Yau, *Singularities and Gauge Theory Phases*, arXiv:1402.6331 [INSPIRE].

[59] M. Esole, S.-H. Shao and S.-T. Yau, *Singularities and Gauge Theory Phases II*, arXiv:1407.1867 [INSPIRE].

[60] A.P. Braun and S. Schäfer-Nameki, *Box Graphs and Resolutions I*, arXiv:1407.3520 [INSPIRE].

[61] P.S. Aspinwall, D.R. Morrison and M. Gross, *Stable singularities in string theory*, *Commun. Math. Phys.* **178** (1996) 115 [hep-th/9503208] [INSPIRE].

[62] A. Grassi, J. Halverson and J.L. Shaneson, *Geometry and Topology of String Junctions*, arXiv:1410.6817 [INSPIRE].

[63] V. Braun and D.R. Morrison, *F-theory on Genus-One Fibrations*, *JHEP* **08** (2014) 132 [arXiv:1401.7844] [INSPIRE].

[64] D.R. Morrison and W. Taylor, *Sections, multisections and* U(1) *fields in F-theory*, arXiv:1404.1527 [INSPIRE].

[65] L.B. Anderson, I. García-Etxebarria, T.W. Grimm and J. Keitel, *Physics of F-theory compactifications without section*, *JHEP* **12** (2014) 156 [arXiv:1406.5180] [INSPIRE].

[66] C. Mayrhofer, E. Palti, O. Till and T. Weigand, *Discrete Gauge Symmetries by Higgsing in four-dimensional F-theory Compactifications*, *JHEP* **12** (2014) 068 [arXiv:1408.6831] [INSPIRE].

[67] D. Klevers, D.K. Mayorga Pena, P.-K. Oehlmann, H. Piragua and J. Reuter, *F-Theory on all Toric Hypersurface Fibrations and its Higgs Branches*, *JHEP* **01** (2015) 142 [arXiv:1408.4808] [INSPIRE].

[68] M. Cvetič, R. Donagi, D. Klevers, H. Piragua and M. Poretschkin, *F-theory vacua with $\mathbb{Z}_3$ gauge symmetry*, *Nucl. Phys.* **B 898** (2015) 736 [arXiv:1502.06953] [INSPIRE].

[69] D. Morrison, D. Park and W. Taylor, to appear.

[70] M. Gross, *A finiteness theorem for elliptic Calabi–Yau threefolds*, *Duke Math. Jour.* **74** (1994) 271.

[71] S. Ashok and M.R. Douglas, *Counting flux vacua*, *JHEP* **01** (2004) 060 [hep-th/0307049] [INSPIRE].

[72] F. Denef and M.R. Douglas, *Distributions of flux vacua*, *JHEP* **05** (2004) 072 [hep-th/0404116] [INSPIRE].

[73] A.P. Braun and T. Watari, *Distribution of the Number of Generations in Flux Compactifications*, *Phys. Rev.* **D 90** (2014) 121901 [arXiv:1408.6156] [INSPIRE].

[74] A.P. Braun and T. Watari, *The Vertical, the Horizontal and the Rest: anatomy of the middle cohomology of Calabi-Yau fourfolds and F-theory applications*, *JHEP* **01** (2015) 047 [arXiv:1408.6167] [INSPIRE].

[75] T. Watari, *Statistics of F-theory flux vacua for particle physics*, *JHEP* **11** (2015) 065 [arXiv:1506.08433] [INSPIRE].

[76] M.R. Douglas and S. Kachru, *Flux compactification*, *Rev. Mod. Phys.* **79** (2007) 733 [hep-th/0610102] [INSPIRE].